# Measurements of inclusive W and Z cross sections in pp collisions at $\sqrt{s} = 7$ TeV

CMS Collaboration ; Amsler, C ; Chiochia, V ; Snoek, H ; Favaro, C ; Verzetti, M ; Aguiló, E ; De Visscher, S ; Schmitt, A ; Millan, B ; Storey, J ; Ivova, M ; Otyugova, P

Abstract: Measurements of inclusive W and Z boson production cross sections in pp collisions at sqrt(s)=7 TeV are presented, based on 2.9 inverse picobarns of data recorded by the CMS detector at the LHC. The measurements, performed in the electron and muon decay channels, are combined to give sigma(pp to WX) times B(W to muon or electron + neutrino) = 9.95 $\pm 0.07(stat.) \pm 0.28(syst.) \pm 1.09(lumi.)nbandsigma(pptoZX)timesB(Ztooppositelychargedmuonorelectronpairs) = 0.931 \pm 0.026(stat.) \pm 0.023(syst.) \pm 0.102(lumi.)nb.Theoreticalpredictions, calculatedatthenext-to-next-to-leadingorderinQCDusingrecer$

DOI: https://doi.org/10.1007/JHEP01(2011)080

EUROPEAN ORGANIZATION FOR NUCLEAR RESEARCH (CERN)

CERN-PH-EP/2010-050
2011/07/24

CMS-EWK-10-002

# Measurements of Inclusive W and Z Cross Sections in pp Collisions at $\sqrt{s} = 7$ TeV

The CMS Collaboration*



## Abstract

Measurements of inclusive W and Z boson production cross sections in pp collisions at $\sqrt{s} = 7$ TeV are presented, based on 2.9 pb$^{-1}$ of data recorded by the CMS detector at the LHC. The measurements, performed in the electron and muon decay channels, are combined to give $\sigma(\mathrm{pp} \to \mathrm{W}X) \times \mathcal{B}(\mathrm{W} \to \ell\nu) = 9.95 \pm 0.07\,(\mathrm{stat.}) \pm 0.28\,(\mathrm{syst.}) \pm 1.09\,(\mathrm{lumi.})$ nb and $\sigma(\mathrm{pp} \to \mathrm{Z}X) \times \mathcal{B}(\mathrm{Z} \to \ell^+\ell^-) = 0.931 \pm 0.026\,(\mathrm{stat.}) \pm 0.023\,(\mathrm{syst.}) \pm 0.102\,(\mathrm{lumi.})$ nb, where $\ell$ stands for either e or $\mu$. Theoretical predictions, calculated at the next-to-next-to-leading order in QCD using recent parton distribution functions, are in agreement with the measured cross sections. Ratios of cross sections, which incur an experimental systematic uncertainty of less than 4%, are also reported.

*Submitted to the Journal of High Energy Physics*

*See Appendix A for the list of collaboration members

# 1 Introduction

The inclusive production of W and Z bosons is an important benchmark process at hadron colliders. Measurements of $\sigma(\mathrm{pp} \to \mathrm{W}X) \times \mathcal{B}(\mathrm{W} \to \ell\nu)$ and $\sigma(\mathrm{pp} \to \mathrm{Z}X) \times \mathcal{B}(\mathrm{Z} \to \ell^+\ell^-)$, where $\ell$ = e or $\mu$, test calculations based on higher-order perturbative QCD and parton distribution functions (PDF). Such calculations are supported by measurements at the $\mathrm{S\overline{p}pS}$ [1, 2] and Tevatron [3–5] $\mathrm{p\overline{p}}$ colliders. We report the extension of these measurements to significantly higher energies, namely, with pp collisions at a center-of-mass energy of 7 TeV provided by the Large Hadron Collider (LHC). The data were collected from April through August, 2010, by the Compact Muon Solenoid (CMS) experiment, and correspond to an integrated luminosity of $(2.88 \pm 0.32)$ pb$^{-1}$. Recently, the ATLAS Collaboration published measurements of cross sections for inclusive W and Z productions at the LHC based on approximately 0.34 pb$^{-1}$ [6]. In this article, "Z boson production" includes $\gamma^*$ exchange within the mass range 60 to 120 GeV.

High-$p_{\mathrm{T}}$ electrons and muons are used for selecting $\mathrm{W} \to \ell\nu$ and $\mathrm{Z} \to \ell^+\ell^-$ candidate events. In addition to a high-$p_{\mathrm{T}}$ lepton, W events are characterized by significant missing transverse energy ($\not\!\!E_{\mathrm{T}}$) due to the escaping neutrino. The reconstruction of electrons and muons is detailed in Section 3, along with lepton identification and isolation requirements, and the $\not\!\!E_{\mathrm{T}}$ reconstruction is described in Section 4.

The measurements of cross sections are based on the formula $\sigma \times \mathcal{B} = N/(A \times \varepsilon \times \mathcal{L})$, where $N$ is the number of signal events, $A$ is the fiducial and kinematic acceptance, $\varepsilon$ is the selection efficiency for events in the acceptance, and $\mathcal{L}$ is the integrated luminosity. The value of $A$ is affected by PDF and renormalization scale uncertainties, while the value of $\varepsilon$ is susceptible to errors from triggering and reconstruction. In order to control the efficiency uncertainties, we concentrate on the extraction of corrections to the efficiencies obtained from the simulation; these correction factors come from efficiency ratios $\rho = \varepsilon/\varepsilon_{\mathrm{sim}}$ derived by measuring $\varepsilon$ and $\varepsilon_{\mathrm{sim}}$ in the same way on data and simulations, respectively. In effect, we replace the product $A \times \varepsilon$ by the product $F \times \rho$, where $F = A \times \varepsilon_{\mathrm{sim}}$ is the fraction of generated events selected in the simulation. The values for $\rho$ are derived from data, and hence their uncertainties are experimental; the uncertainties on $F$ derive from the theoretical uncertainties on $A$. In order to exploit this distinction between experimental and theoretical uncertainties, we also report cross section measurements defined within the restricted acceptance dictated by the detector coverage and minimum transverse momentum; these values incur essentially no theoretical uncertainty.

In Section 5 we determine electron and muon selection efficiency correction factors from the data. The selection of events for the W and Z samples and the extraction of signal event yields are outlined in Section 6, followed by a discussion of systematic uncertainties in Section 7. Finally, the results are reported and briefly discussed in Section 8.

In the following section, a brief description of the CMS detector is provided.

# 2 The CMS detector

The central feature of the CMS apparatus is a superconducting solenoid of 6 m internal diameter, providing a magnetic field of 3.8 T. Within the field volume are a silicon pixel and strip tracker, an electromagnetic calorimeter (ECAL) and a brass/scintillator hadron calorimeter (HCAL). Muons are detected in gas-ionization detectors embedded in the steel return yoke. In addition to the barrel and endcap detectors, CMS has extensive forward calorimetry.

CMS uses a right-handed coordinate system, with the origin at the nominal interaction point,

the $x$-axis pointing to the center of the LHC ring, the $y$-axis pointing up (perpendicular to the LHC plane), and the $z$-axis along the anticlockwise-beam direction. The polar angle $\theta$ is measured from the positive $z$-axis and the azimuthal angle $\phi$ is measured in radians in the $xy$-plane. The pseudorapidity is given by $\eta = -\ln(\tan\theta/2)$.

The inner tracker measures charged particle trajectories in the pseudorapidity range $|\eta| < 2.5$. It consists of 1 440 silicon pixel and 15 148 silicon strip detector modules. It provides an impact parameter resolution of $\sim 15\,\mu$m and a transverse momentum ($p_T$) resolution of better than 1% for charged particles with $p_T$ above 40 GeV.

The electromagnetic calorimeter consists of nearly 76 000 lead tungstate crystals which provide coverage in pseudorapidity $|\eta| < 1.479$ in a cylindrical barrel region (EB) and $1.479 < |\eta| < 3.0$ in two endcap regions (EE). A preshower detector consisting of two planes of silicon sensors interleaved with a total of 3 $X_0$ of lead is located in front of the EE. The ECAL has an ultimate energy resolution of better than 0.5% for unconverted photons with transverse energies above 100 GeV. The energy resolution is 3% or better for the range of electron energies relevant for this analysis. The hadronic calorimeter is a sampling device with brass as passive material and scintillator as active material. The combined calorimeter cells are grouped in projective towers of granularity $\Delta\eta \times \Delta\phi = 0.087 \times 0.087$ at central rapidities and $0.175 \times 0.175$ at forward rapidities.

Muons are detected in the pseudorapidity window $|\eta| < 2.4$, with detection planes based on three technologies: drift tubes, cathode strip chambers, and resistive plate chambers. A high-$p_T$ muon originating from the interaction point produces track segments in typically three or four muon stations. Matching these segments to tracks measured in the inner tracker results in a $p_T$ resolution between 1 and 2% for $p_T$ values up to 100 GeV.

The first level (L1) of the CMS trigger system, composed of custom hardware processors, is designed to select the most interesting events in less than 1 $\mu$s using information from the calorimeters and muon detectors. The High Level Trigger (HLT) processor farm further decreases the event rate to a few hundred hertz, before data storage.

A more detailed description of CMS can be found elsewhere [7].

## 3 Lepton Reconstruction and Identification

Events in which hadronic jets mimic an electron or a muon can contaminate the W and Z samples. Such fake leptons, as well as real leptons arising from decays of heavy-flavour hadrons or decays in flight of light mesons within jets, are suppressed by imposing limits on additional energy recorded near the projected impact point of the candidate lepton in the calorimeters, as well as on the energy of charged particles reconstructed in the inner tracker near the direction of the candidate lepton. We define isolation variables for the three subsystems: $I^{\rm rel}_{\rm ECAL} = \sum E_T({\rm ECAL})/p^\ell_T$, $I^{\rm rel}_{\rm HCAL} = \sum E_T({\rm HCAL})/p^\ell_T$ and $I^{\rm rel}_{\rm trk} = \sum p_T({\rm tracks})/p^\ell_T$, where $p^\ell_T$ is the transverse momentum of the lepton candidate. The scalar sums of transverse energy ($E_T$) and transverse momentum ($p_T$) are performed for objects falling within a cone $\Delta R = \sqrt{(\Delta\eta)^2 + (\Delta\phi)^2} < 0.3$ around the lepton candidate, the energy deposits and the track associated with the lepton candidate being excluded from the sums. We also define a combined isolation variable, $I^{\rm rel}_{\rm comb} = I^{\rm rel}_{\rm ECAL} + I^{\rm rel}_{\rm HCAL} + I^{\rm rel}_{\rm trk}$.

## 3.1 Electrons

Events with high-$E_T$ electrons are selected online when they pass a L1 trigger filter that requires a coarse-granularity region of the ECAL to have $E_T > 5$ GeV. They subsequently must pass an HLT [8] filter that requires an ECAL cluster with $E_T > 15$ GeV, using the full granularity of the ECAL and $E_T$ measurements corrected using offline calibration [9].

Electrons are identified offline as clusters of ECAL energy deposits matched to tracks from the silicon tracker. The ECAL clusters are designed to collect the largest fraction of the energy of the original electron, including energy radiated along its trajectory. They must fall in the ECAL fiducial volume of $|\eta| < 1.44$ for EB clusters or $1.57 < |\eta| < 2.5$ for EE clusters. The transition region from $1.44 < |\eta| < 1.57$ is excluded as it leads to lower-quality reconstructed clusters, due mainly to services and cables exiting between the barrel and endcap calorimeters. Electron tracks are reconstructed using an algorithm [10] that accounts for possible energy loss due to bremsstrahlung in the tracker layers. Particles misidentified as electrons are suppressed by requiring that the $\eta$ and $\phi$ coordinates of the track trajectory extrapolated to the ECAL match the $\eta$ and $\phi$ coordinates of the ECAL cluster, by requiring a narrow ECAL cluster width in $\eta$, and by limiting the HCAL energy measured in a cone of $\Delta R < 0.15$ around the ECAL cluster direction.

Electrons from photon conversions are suppressed by requiring one hit in the innermost pixel layer for the reconstructed electron track. Furthermore, electrons are rejected when a partner track is found that is consistent with a photon conversion, based on the opening angle and the separation in the transverse plane at the point at which the electron and partner tracks are parallel.

For both the W and Z analyses an electron candidate is considered isolated if $I^{\text{rel}}_{\text{trk}} < 0.09$, $I^{\text{rel}}_{\text{ECAL}} < 0.07$ and $I^{\text{rel}}_{\text{HCAL}} < 0.10$ in the barrel region; $I^{\text{rel}}_{\text{trk}} < 0.04$, $I^{\text{rel}}_{\text{ECAL}} < 0.05$ and $I^{\text{rel}}_{\text{HCAL}} < 0.025$ in the endcap regions.

The electron selection criteria were obtained by optimizing signal and background levels according to simulation-based studies. The optimization was done for EB and EE separately. We use the same criteria for the $W \to e\nu_e$ and $Z \to e^+e^-$ channels; these select approximately 75% of the reconstructed electrons in the data with clusters in the ECAL fiducial volume and $E_T > 20$ GeV, and reduce the fake electron background by two orders of magnitude.

More details and studies of electron reconstruction and identification can be found in Ref. [11].

## 3.2 Muons

Events with high-$p_T$ muons are selected online if the data from the muon chambers satisfy the L1 muon trigger, and if a muon candidate reconstructed from both muon chamber and tracker data satisfies the HLT. An HLT threshold of $p_T > 9$ GeV for muons in the range $|\eta| < 2.1$ is chosen as the baseline for the analysis.

Offline, a number of quality requirements are imposed. Muon candidates can be reconstructed by two different algorithms: one starts from inner-tracker information ("tracker muons"), and another starts from segments in the muon chambers ("global muons"). We demand that muon candidates for this analysis be reconstructed by both algorithms. We also demand signals in at least two muon stations, and require that $\chi^2/N_{\text{dof}} < 10$ for a global fit containing all valid tracker and muon hits, where $N_{\text{dof}}$ is the number of degrees of freedom. The first condition ensures a sensible momentum estimate at the muon trigger level, and further suppresses remaining punch-through and sail-through hadrons. The second condition suppresses contributions

from light-meson decays-in-flight.

In order to ensure a precise estimate of momentum and impact parameter, only tracks with more than 10 hits in the tracker and at least one hit in the pixel detector are used. Cosmic-ray muons are rejected by requiring an impact parameter relative to the nominal beam axis of less than 2 mm. Studies of cosmic-ray muons confirm that the high-$p_{\mathrm{T}}$ cosmic muon contamination is negligible.

As in the case of electrons, isolation criteria are applied. For both W and Z analyses, a muon candidate is considered isolated if $I^{\mathrm{rel}}_{\mathrm{comb}} < 0.15$.

More details and studies of muon reconstruction and identification can be found in Ref. [12].

## 4 Missing Transverse Energy

An accurate $\not\!\!E_{\mathrm{T}}$ measurement is essential for distinguishing a W signal from QCD multijet production backgrounds. We profit from the application of the particle flow (PF) algorithm [13], which provides superior $\not\!\!E_{\mathrm{T}}$ reconstruction performance at the energy scale of W boson production. The algorithm combines information from the inner tracker, the muon chambers, and all the calorimetry cells to classify reconstructed objects according to particle type (electron, muon, photon, charged or neutral hadron), thereby allowing precise energy corrections, and also providing a significant degree of redundancy that reduces the sensitivity of the $\not\!\!E_{\mathrm{T}}$ measurements to miscalibrations of the calorimetry.

Anomalous noise signals can spoil the $\not\!\!E_{\mathrm{T}}$ measurements. A dedicated effort to identify and remove such noise in the ECAL and HCAL, based on cosmic-ray and control samples as well as collision data, has successfully reduced the impact of such noise to a negligible level; there is no discernible difference in the $\not\!\!E_{\mathrm{T}}$ distributions for $W \to \ell\nu$ events from data and from simulation [14].

The $\not\!\!E_{\mathrm{T}}$ is the modulus of the transverse missing momentum vector, computed as the negative of the vector sum of all reconstructed transverse momenta of particles identified with the PF algorithm. The $\not\!\!E_{\mathrm{T}}$ resolution for inclusive multijet samples and for $W \to \ell\nu$ events is reproduced well by the simulation. The resolution worsens by about 10% when there is more than one primary vertex; this occurs in about 40% of the events in the considered data set, and has a negligible impact on the extraction of the W signal yields described below.

## 5 Lepton Selection Efficiencies

The efficiencies for lepton reconstruction, identification, isolation and trigger efficiencies are obtained from data. Correction factors for the values extracted from the simulation are determined with a tag-and-probe method exercised on $\mathrm{Z} \to \ell^+\ell^-$ samples in both data and simulation. This procedure adequately removes any systematic uncertainties coming from imperfections in the simulation, even though the kinematic distributions of leptons in the $\mathrm{Z} \to \ell^+\ell^-$ sample differ slightly from those in the selected $\mathrm{W} \to \ell\nu$ sample.

The tag-and-probe sample for the measurement of a given efficiency contains events selected with two lepton candidates. One lepton candidate, called the "tag," satisfies tight identification and isolation requirements. The other lepton candidate, called the "probe," is selected with criteria that depend on the efficiency being measured. The invariant mass of the tag and probe lepton candidates must fall in the range 60–120 GeV. The signal yields are obtained for two exclusive subsamples of events in which the probe lepton passes or fails the selection

criteria considered. Fits are performed to the invariant-mass distributions of the pass and fail subsamples, including a term that accounts for the background. The measured efficiency is deduced from the relative level of signal in the pass and fail subsamples; its uncertainty includes a systematic contribution from the fitting procedure.

The correction factors are obtained as ratios of tag-and-probe efficiencies for the data and for the simulation. They are used to compute the signal selection efficiency ratios $\rho$, and their uncertainties are propagated as systematic uncertainties on these quantities, except in the $Z \to \mu^+\mu^-$ analysis, for which the efficiencies and yields are determined simultaneously.

The efficiency of the lepton isolation requirements can also be measured using a "random-cone" technique. In the inclusive W or Z sample, energy contributing to the isolation variables comes mainly from the underlying event, which can be sampled in directions uncorrelated with the lepton directions in a particular event. We use leptons in simulated signal events to define directions in data events where the isolation energies can be measured and compared to the requirements of the analysis; this ensures a sampling of phase space that mimics the leptons in real data events. Studies with simulation verify that this technique provides values for the isolation efficiency that are accurate to about 0.5% for muons and 1% for electrons.

## 5.1 Electrons

The electron selection efficiency is the product of three components: 1) the reconstruction efficiency, 2) the identification and isolation efficiency, and 3) the trigger efficiency. Efficiencies are evaluated for the barrel and endcap regions, and for the two possible electron charges, separately.

The reconstruction efficiency is the probability of finding a reconstructed track when the electron cluster is within the ECAL fiducial volume. The probe is selected as an ECAL cluster of reconstructed transverse energy greater than 20 GeV. To reduce backgrounds, which are not insignificant, we use a tight selection on the tag and require the probe to pass additional loose shower shape and isolation requirements; these are known from simulations to be uncorrelated with the reconstruction efficiency. The measured reconstruction efficiency is the fraction of probes reconstructed as electron tracks. For the EB and EE electrons we measure a reconstruction efficiency of $(98.6 \pm 0.5)\%$ and $(96.2 \pm 0.8)\%$, respectively. The resulting correction factors are consistent with unity.

The efficiency of electron identification, isolation, and conversion rejection requirements is estimated relative to the sample of reconstructed electrons. The tag selection does not need to be tight, and no additional criteria on the probe are imposed. In the barrel, we measure a selection efficiency of $(79.1 \pm 1.8)\%$, to be compared to 85.5% for the simulation, resulting in a correction factor of $0.925 \pm 0.021$. In the endcaps, an efficiency of $(69.2 \pm 2.0)\%$ is measured, where 74.9% is expected from simulation, resulting in a correction factor of $0.924 \pm 0.027$. The random-cone technique is used to cross check the efficiency of the electron isolation requirements. The results confirm the values within 1.0% for EB and 1.8% for EE electrons, respectively.

Finally, we obtain combined L1 and HLT trigger efficiencies from identified and isolated electron candidates as probes. We measure $(98.9 \pm 0.3)\%$ in the barrel, and $(99.2 \pm 0.5)\%$ in the endcaps, leading to correction factors consistent with unity. These tag-and-probe efficiencies are confirmed by measurements made with a sample of minimum-bias events selected with scintillation counters and a sample of events selected by an HLT algorithm that has minimum-bias requirements at L1 and a complete emulation of the offline ECAL cluster reconstruction.

The charge misidentification for electrons in the simulated W sample is $(0.67 \pm 0.01)\%$. We

infer a data/simulation charge misidentification correction factor of $1.2^{+0.4}_{-0.3}$ by comparing the fraction of events with electrons of same electric charge in data and simulation samples. This correction factor is included in the results for $W^{\pm}$ cross sections, as well as their ratio, and its error propagated to the systematic uncertainties on these quantities.

The products of all correction factors for the electron selection are $0.919 \pm 0.022$ for the EB and $0.926 \pm 0.028$ for the EE.

When combining the correction factors, we take into account the relative acceptance of electrons from W decays in the EB and EE. We obtain the efficiency ratio for $W \to e\nu_e$ events: $\rho_W = 0.921 \pm 0.036$; and separately by charge: $\rho_{W^+} = 0.917 \pm 0.046$ and $\rho_{W^-} = 0.927 \pm 0.047$. We infer a signal selection efficiency of $(72.1 \pm 2.8)\%$ for $W \to e\nu_e$ events with the electron cluster in the ECAL fiducial volume and $E_T > 20$ GeV.

In the $Z \to e^+e^-$ analysis, one electron candidate is allowed to fail the trigger criteria; the efficiency ratio is $\rho_Z = 0.856 \pm 0.050$ and the corrected signal selection efficiency for $Z \to e^+e^-$ events with both electron clusters in ECAL fiducial volume and $E_T > 20$ GeV is $(56.2 \pm 3.3)\%$.

## 5.2 Muons

The muon reconstruction and selection efficiency has five distinguishable components: 1) the efficiency to find a track in the inner tracker, 2) the efficiency to find a track in the muon chambers, and, for a muon candidate, 3) the efficiency to pass the quality requirements, 4) the efficiency to pass the isolation requirements, and 5) the probability to pass the L1 trigger and HLT.

Muon efficiencies are extracted from the sample of candidate $Z \to \mu^+\mu^-$ events. The tag muon must pass all muon selection criteria. The invariant mass of the tag-and-probe muon candidates is formed; invariant-mass distributions are produced for exclusive categories of events where the probe muon passes or fails various efficiency requirements. Simultaneous fits to those distributions allow the number of signal events and the efficiencies to be extracted.

The inner-tracker efficiency is studied using well-reconstructed tracks in the muon chambers as probes. The efficiency for tracking in the muon chambers is tested with tracker muons satisfying very loose matching to muon track segments. To measure the efficiency of quality requirements, the probe muon must pass all the selection criteria except those on the $\chi^2$ and on the impact distance to the beam axis. Finally, the isolation efficiency is measured using muons that pass the quality requirements, and the trigger efficiency using muons that in addition are isolated.

The following efficiencies are obtained: for inner tracking, $(99.1 \pm 0.4)\%$; for muon tracking, $(96.4 \pm 0.5)\%$; for quality requirements, $(99.7 \pm 0.3)\%$; for isolation, $(98.5 \pm 0.4)\%$; and for trigger, $(88.3 \pm 0.8)\%$. All correction factors are consistent with unity, except for the trigger efficiency, for which the correction factor is $0.947 \pm 0.009$.

Isolation efficiencies have also been measured using the random-cone technique, and the results confirm the tag-and-probe value for the isolation efficiency quoted above: 98.7% for $W \to \mu\nu_\mu$ and 98.5% for $Z \to \mu^+\mu^-$.

The overall muon selection efficiency is $(82.8 \pm 1.0)\%$, to be compared to the value of 88.7% obtained from the simulation; the efficiency ratio is $\rho_W = 0.933 \pm 0.012$. There is no significant difference between the efficiency ratios for positive and negative muons: $\rho_{W^+} = 0.935 \pm 0.018$ and $\rho_{W^-} = 0.931 \pm 0.019$, respectively.

# 6 Event Selection and Signal Extraction

The data used for these measurements were collected from April to August 2010. We used only those data-taking periods passing the standard CMS quality criteria, which allow no anomalous or faulty behavior for the inner tracker, the calorimeters, and the muon chambers.

Several large samples of simulated events were used to evaluate the signal and background efficiencies and to validate our analysis techniques. Samples of electroweak processes with W and Z production, both for signal and background events, were produced with POWHEG [15–17], interfaced with the PYTHIA [18] parton-shower generator. QCD events with muons, electrons, or jets likely to be misidentified as electrons in the final state were studied with PYTHIA, as were other minor backgrounds such as $\mathrm{t\bar{t}}$ and certain electroweak processes ($\mathrm{W} \to \tau\nu_\tau$, $\mathrm{Z} \to \tau^+\tau^-$, WW, WZ, and ZZ). We do not consider the diboson channels (WW, WZ, and ZZ) as part of the W and Z signals in order to facilitate the comparison of our results to theoretical predictions, which do not take these contributions into account. Generated events were processed through the full GEANT4 [19] detector simulation, trigger emulation, and event reconstruction chain.

## 6.1 W boson selection

The W events are characterized by a prompt, energetic, and isolated lepton, and significant missing energy. The main backgrounds are QCD multijet events and Drell-Yan events in which one lepton fails the selection. The QCD background is reduced by requiring the lepton to be isolated; the remaining events do not have large $\not\!\!E_\mathrm{T}$ and can be distinguished from signal events on a statistical basis. The Drell-Yan background is suppressed by rejecting events with a second lepton candidate.

To measure the signal yields, we choose to fit the $\not\!\!E_\mathrm{T}$ distribution in the electron channel and the $M_\mathrm{T}$ distribution in the muon channel, where $M_\mathrm{T} = \sqrt{2p_\mathrm{T}\not\!\!E_\mathrm{T}(1-\cos\Delta\phi)}$; $\Delta\phi$ is the angle between the missing transverse momentum and the lepton transverse momentum. QCD backgrounds are estimated from data, as explained below. According to the simulation, $\mathrm{W} \to \tau\nu_\tau$ makes a small relative contribution; backgrounds from $\mathrm{Z} \to \tau^+\tau^-$, $\mathrm{t\bar{t}}$, and diboson production are negligible in both electron and muon channels.

### 6.1.1 Electrons

The $\mathrm{W} \to \mathrm{e}\nu_\mathrm{e}$ candidate events are required to have one identified electron with an ECAL cluster of $E_\mathrm{T} > 20\,\mathrm{GeV}$ in the ECAL fiducial volume. If a second electron candidate satisfying looser criteria and with $E_\mathrm{T} > 20\,\mathrm{GeV}$ is present in the event, the event is rejected. The fraction of signal events selected in the simulation is $F_\mathrm{W} = 0.446 \pm 0.006$, with $F_{\mathrm{W}^+} = 0.459 \pm 0.007$ and $F_{\mathrm{W}^-} = 0.428 \pm 0.008$. The number of events selected in the data is 28 601, with 15 859 positive and 12 742 negative electrons.

The $\mathrm{W} \to \mathrm{e}\nu_\mathrm{e}$ signal is extracted from an unbinned maximum likelihood fit of the observed $\not\!\!E_\mathrm{T}$ distribution to the sum of signal and background shapes. The QCD background shape, which accounts for both QCD multijet production and direct-photon production with the photon converting in the detector, can be modeled by a modified Rayleigh distribution,

$$f(\not\!\!E_\mathrm{T}) = \not\!\!E_\mathrm{T} \times \exp\left(-\frac{\not\!\!E_\mathrm{T}^2}{2(\sigma_0+\sigma_1\not\!\!E_\mathrm{T})^2}\right).$$

This function can be understood as describing fluctuations of the missing transverse momentum vector around zero due to measurement errors; the resolution term, $\sigma_0 + \sigma_1\not\!\!E_\mathrm{T}$, increases

with $\not\!\!E_T$ to account for tails in the $\not\!\!E_T$ measurement. This function describes well the QCD background shape in the simulation, over the full range of $\not\!\!E_T$, as well as $\not\!\!E_T$ distributions from signal-free samples obtained by inverting the identification or isolation criteria.

The signal distributions are derived from simulation, separately for $W^+$ and $W^-$, and receive an event-by-event correction in bins of the W transverse momentum, determined from a study of the hadronic recoil distributions of $Z \to e^+e^-$ events in the data [14]. In fits to the $\not\!\!E_T$ distributions, the free parameters are the W signal yield, the QCD background yield, and the shape parameters $\sigma_0$ and $\sigma_1$.

We extract the inclusive yield $N_W$ from a fit where the expected ratio for $\sigma_{W^+}/\sigma_{W^-}$ is assumed. It has been checked that the result was insensitive to this assumption. Figure 1 (a) shows the $\not\!\!E_T$ distribution of the inclusive $W \to e\nu_e$ sample and the results of the likelihood fit; the fit function describes the data well, with a $p$-value of 0.49 for the Kolmogorov-Smirnov test. The inclusive yield is $N_W = 11\,895 \pm 115$ events.

The signals for the $W^+ \to e^+\nu_e$ and $W^- \to e^-\overline{\nu}_e$ channels are extracted from a simultaneous fit to the individual $\not\!\!E_T$ distributions, in which the QCD background shape parameters $\sigma_0$ and $\sigma_1$ are constrained to be the same for both samples. The yields are $N_{W^+} = 7\,193 \pm 89$ for $W^+ \to e^+\nu_e$ and $N_{W^-} = 4\,728 \pm 73$ for $W^- \to e^-\overline{\nu}_e$, with a negligible correlation. Because the two fits are independent, the relation $N_W = N_{W^+} + N_{W^-}$ is not exactly satisfied, but holds to within 0.2%.

### 6.1.2 Muons

The $W \to \mu\nu_\mu$ candidate events are required to have a muon with $p_T > 20$ GeV and $|\eta| < 2.1$. If a second muon with $p_T > 10$ GeV is present, the event is rejected in order to reduce the contribution from Drell-Yan events. The fraction of signal events selected from the simulation is $F_W = 0.462 \pm 0.005$, with $F_{W^+} = 0.477 \pm 0.005$ and $F_{W^-} = 0.441 \pm 0.005$. The number of selected events is 18 571, including 10 682 with positive and 7 889 with negative muons.

The $W \to \mu\nu_\mu$ signal yield is extracted from a binned likelihood fit to the observed $M_T$ distribution, which is taken to be the sum of different contributions: $W \to \mu\nu_\mu$ signal, QCD background, electroweak (EWK) backgrounds, and $t\bar{t}$. The shapes of the signal and background components (templates) are taken from the simulation, except for the QCD background, which is obtained from data, as described below. The normalization of the QCD background and the $W \to \mu\nu_\mu$ yield are free parameters in the fit. The EWK and $t\bar{t}$ backgrounds are normalized to the $W \to \mu\nu_\mu$ yield on the basis of simulations and expected relative cross sections.

The QCD template used in the fit is obtained from a high-purity QCD sample referred to as the inverted sample. This sample is selected by applying the same criteria as in the signal selection except the isolation requirement, which is reversed: $I^{\text{rel}}_{\text{comb}} > 0.20$. The shape of the QCD template from the inverted sample in the data agrees well with that obtained in the simulation. Studies of simulated QCD events show that a small bias in the shape is induced by the isolation requirement. This bias comes from the correlation of the isolation variable with the $\sum E_T$ in the event. We correct the template on the basis of a linear relation between $M_T$ and $I^{\text{rel}}_{\text{comb}}$. In the simulation, we obtain an excellent match between the corrected template from the inverted sample and the actual template from the non-inverted sample. We compare the yields obtained when fitting with different QCD templates, namely, corrected template in the data and uncorrected templates obtained from the inverted sample in the data and from the non-inverted sample in the simulation. We take the maximum difference in yields as an estimate of the systematic uncertainty from the modeling of the QCD background shape.

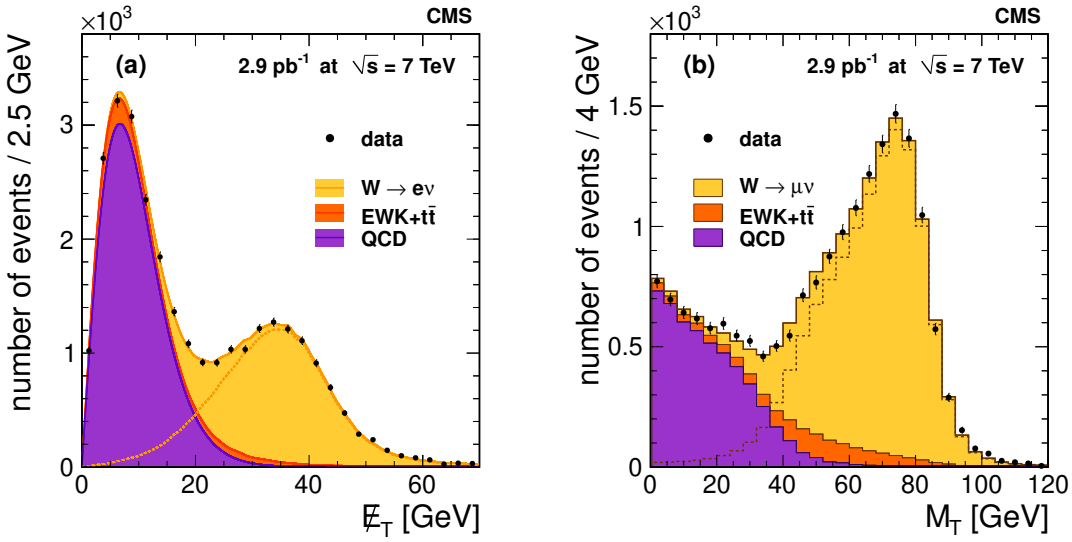


Figure 1: The W signal distributions: (a) $\not\!\!E_T$ distribution for the selected $W \to e\nu_e$ sample; (b) $M_T$ distributions for the selected $W \to \mu\nu_\mu$ sample. The points represent the data. Superimposed are the results of the maximum likelihood fits for signal plus backgrounds, in yellow; all backgrounds, in orange; QCD backgrounds, in violet. The dashed lines represent the signal distributions.

As in the case of electrons, the signal template receives an event-by-event correction in bins of the W transverse momentum determined from a study of the hadronic recoil distributions of $Z \to \mu^+\mu^-$ events in the data.

Figure 1 (b) shows the fit to the observed $M_T$ spectrum of the inclusive $W \to \mu\nu_\mu$ sample; the fit distribution describes the data well, with a $p$-value of 0.34 for the Kolmogorov-Smirnov test. The inclusive yield is $N_W = 12\,257 \pm 111$. The charge-specific yields are $N_{W^+} = 7\,445 \pm 87$ and $N_{W^-} = 4\,812 \pm 69$. Here, we fit simultaneously for the inclusive yield $N_W$ and the ratio $N_{W^+}/N_{W^-}$ so that, by construction, $N_W = N_{W^+} + N_{W^-}$.

## 6.2 Z boson selection

To identify $Z \to \ell^+\ell^-$ decays, a pair of identified leptons is required, with dilepton invariant mass in the range $60 < M_{\ell^+\ell^-} < 120$ GeV. Backgrounds are very low, including backgrounds from QCD processes. In the $Z \to e^+e^-$ channel, the yield is obtained by counting the number of selected events and making a small correction for backgrounds. In the $Z \to \mu^+\mu^-$ channel, yield and lepton efficiencies are fitted simultaneously. No correction is made for $\gamma^*$ exchange.

### 6.2.1 Electrons

The $Z \to e^+e^-$ candidate events are required to have two electrons satisfying the same selection criteria as the electrons selected in the $W \to e\nu_e$ sample. Both electrons must have an ECAL cluster with $E_T > 20$ GeV in the ECAL fiducial volume. The fraction of signal events selected in the simulation is $F_Z = 0.285 \pm 0.005$.

The Z mass peaks in the data exhibit small shifts, on the order of 1 to 2%, with respect to the simulated distributions. From these shifts, we determine ECAL cluster energy scale correction factors of $1.015 \pm 0.002$ and $1.033 \pm 0.005$ for barrel and endcap electrons, respectively. The uncertainties on these correction factors are propagated as systematic uncertainties on the yield.

Applying these corrections to electron candidates in the data, we select 677 events, with the dielectron invariant mass shown in Fig. 2 (a), along with the predicted distribution, after the energy scale correction of the data and normalization of the simulation.

Three techniques are used to estimate the background originating from events in which one or both electron candidates are misidentified jets or photons. The first method measures the probability of jets to be misidentified as electron from a large sample of events selected with a jet trigger. The second method is based on counting events with electron candidates of same electric charge, after taking into account the probability of wrong charge assignment. The third method uses a fit to the track isolation variable to extract the fractions of signal and QCD background. The three methods are independent and give consistent results. Combining them, we estimate the QCD background in our sample to be $0.4 \pm 0.4$ events. Backgrounds from other processes with true electrons ($Z \to \tau^+\tau^-$, dibosons, and $t\bar{t}$) are estimated from the simulation. The total background in the $Z \to e^+e^-$ sample is estimated to be $2.8 \pm 0.4$ events.

### 6.2.2 Muons

In the $Z \to \mu^+\mu^-$ channel, event yields and muon selection efficiencies are extracted from a simultaneous fit. The tag-and-probe sample is built from events containing two muon candidates with $p_T > 20$ GeV and $|\eta| < 2.1$. The tag muon satisfies the identification and isolation criteria used in the $W \to \mu\nu_\mu$ selection; the probe muon is selected as either a tracker or global muon. The tag-and-probe sample is divided into five mutually-exclusive samples of events, according to the quality of the probe muon, as described above. In the signal sample, the probe muon fulfills all the identification and isolation criteria, and at least one of the muon candidates satisfies the trigger requirement. This sample contains 913 events. The distribution of the dimuon invariant mass is shown in Fig. 2 (b), compared with distributions based on simulations normalized to the measured cross section.

The background is negligible in the signal sample. The mass spectrum in that sample is used as a model for the signal shapes in other samples, where backgrounds are modeled by products of a polynomial and an exponential function. The yields and efficiencies are extracted from a joint binned maximum likelihood fit to all mass spectra. The $Z \to \mu^+\mu^-$ signal yield is already corrected for efficiency by virtue of the parameterization used in the fit; the corrected yield is $N_Z/\varepsilon_Z = 1\,050 \pm 35$ events and the signal acceptance is $A_Z = 0.398 \pm 0.005$.

The muon momentum scale and resolution are verified in different $p_T$ regions from the study of lower-mass dimuon resonances ($J/\psi$ and $\Upsilon$), the cosmic-ray muon endpoint [20], the matching of tracker muons and global muons, the W transverse momentum spectrum, and the Z mass lineshape. From the observed agreements with the simulation, we find that no momentum corrections are needed.

The QCD multijet background in the signal sample is estimated to be $0.048 \pm 0.002$ event. Including or neglecting this background in the simultaneous fit changes the yield by 0.2%, which we take as a systematic uncertainty on the background. A further systematic uncertainty stems from the modeling of the shapes of signal and background; we estimate this uncertainty to be 1%. The contributions from other backgrounds ($Z \to \tau^+\tau^-$, dibosons, and $t\bar{t}$) are small, according to simulations, and amount to $3.5 \pm 0.2$ events in total.

## 7 Systematic Uncertainties

The largest uncertainty for the cross section measurement comes from the estimation of the integrated luminosity. CMS uses signals from the forward hadronic (HF) calorimeters to mea-

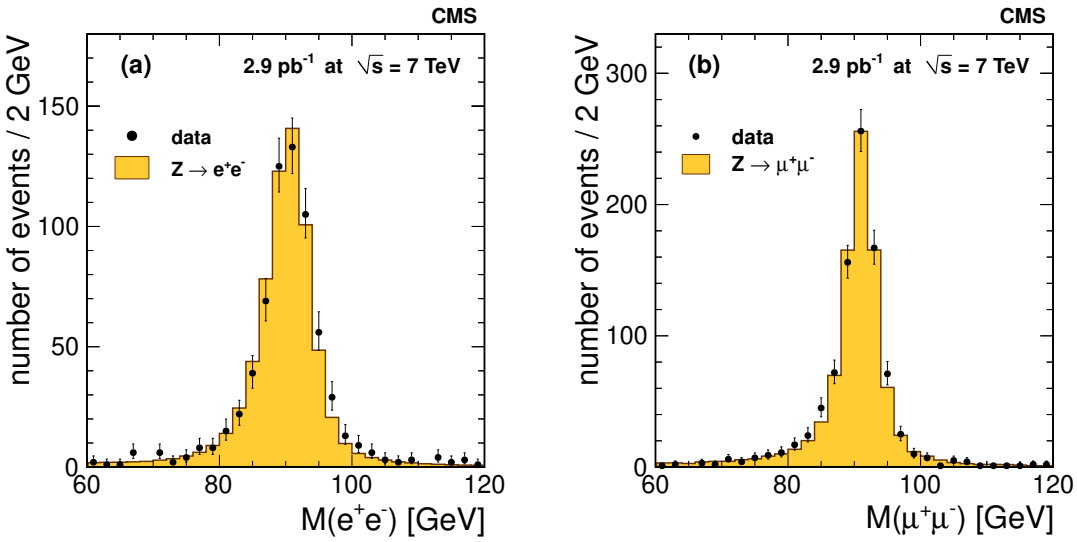


Figure 2: The Z signal distributions: (a) dielectron mass spectrum for the selected $Z \to e^+e^-$ sample; (b) dimuon mass spectrum for the selected $Z \to \mu^+\mu^-$ sample. The points represent the data and the histograms, the simulation. Backgrounds are negligible and are not represented in the plots.

sure the instantaneous luminosity in real time with an absolute normalization obtained with Van der Meer scans, from which we infer the size of the colliding beams and thereby the luminosity, with minimal reliance on simulations [21]. The total luminosity uncertainty amounts to 11% and is expected to diminish in the future.

Aside from luminosity, the main source of experimental uncertainty in our measurements comes from the propagation of uncertainties on the efficiency ratios obtained by the tag-and-probe method. This amounts to 3.9% and 1.4% for $W \to e\nu_e$ and $W \to \mu\nu_\mu$ analyses, respectively. In the $Z \to e^+e^-$ channel, we conservatively neglect the anti-correlation between efficiencies and yields, which are extracted separately from the same sample; the efficiency uncertainties amount to 5.9%. In the $Z \to \mu^+\mu^-$ analysis, yield and efficiencies are determined simultaneously, and therefore the efficiency uncertainties are part of the statistical error from the fit. Corrections of 0.5% and 1.0% are applied to the $W \to \mu\nu_\mu$ and $Z \to \mu^+\mu^-$ event yields, respectively, to account for a loss of events due to barrel muon triggers that failed timing requirements and for which the tracker data were not read out properly. These corrections are determined from the data, and lead to a 0.5% systematic uncertainty in both channels.

Sub-dominant systematic uncertainties come from the lepton energy/momentum scale and resolution. Electron energy correction factors are approximately 1% to 3% in the barrel and endcap calorimeters, from the observed shift of the Z mass peak. In the $W \to e\nu_e$ case, the electron energy scale has an impact on the $\not\!\!E_T$ distribution for the signal; we apply typical energy scale corrections to electrons in the simulation (before $E_T$ threshold selection) and recompute the $\not\!\!E_T$. From variations of the signal yields from the fit, we assign a 2.0% systematic uncertainty to the $W \to e\nu_e$ cross section. In the $Z \to e^+e^-$ analysis, the $E_T$ threshold and mass window requirements lead to a 0.6% uncertainty due to the energy scale uncertainty. Studies of the $Z \to \mu^+\mu^-$ line shape show that data/simulation momentum scale shifts larger than 0.4% can be excluded, which imply small uncertainties of 0.3% in the $W \to \mu\nu_\mu$ analysis, and 0.2% in the $Z \to \mu^+\mu^-$ analysis.

Table 1: Systematic uncertainties of the four cross section measurements, in percent. "n/a" means the source does not apply. A common luminosity uncertainty of 11% applies to all channels.

| Source | $W \to e\nu_e$ | $W \to \mu\nu_\mu$ | $Z \to e^+e^-$ | $Z \to \mu^+\mu^-$ |
|---|---|---|---|---|
| Lepton reconstruction & identification | 3.9 | 1.5 | 5.9 | 0.5 |
| Momentum scale & resolution | 2.0 | 0.3 | 0.6 | 0.2 |
| $\not\!\!E_T$ scale & resolution | 1.8 | 0.4 | n/a | n/a |
| Background subtraction/modeling | 1.3 | 2.0 | 0.1 | $0.2 \oplus 1.0$ |
| PDF uncertainty for acceptance | 0.8 | 1.1 | 1.1 | 1.2 |
| Other theoretical uncertainties | 1.3 | 1.4 | 1.3 | 1.6 |
| Total | 5.1 | 3.1 | 6.2 | 2.3 |

The $\not\!\!E_T$ energy scale is affected by our limited knowledge of the intrinsic hadronic recoil response. We observe minor discrepancies when comparing hadronic recoil distributions in data and simulation, and assign an uncertainty of 1.8% in the $W \to e\nu_e$ analysis due to the $\not\!\!E_T$ energy scale. In the muon channel, this uncertainty is estimated by refitting the $M_T$ distribution with the signal shape predicted by the simulation. The variation in the signal yield with respect to the reference result is 0.4%.

In the $W \to e\nu_e$ channel, the systematic uncertainty due to background subtraction is obtained by comparing fits to various background-dominated distributions: the sample selected with inverted identification criteria in the data, and the samples selected with and without inverted identification criteria in the QCD simulation. We quantify the differences in the tails of these three distributions by an extra parameter in our analytical background function. Using a set of pseudo-experiments to estimate the impact of such differences on the results of the nominal fit, we evaluate the uncertainty due to background subtraction in the $W \to e\nu_e$ analysis to be 1.3%. In the $W \to \mu\nu_\mu$ analysis the QCD background shape is tested by refitting the $M_T$ spectrum with the background shape fixed to QCD-enriched sample expectations. This choice provides the maximum variation (2.0%) in the signal yield with respect to the reference fit.

The background from fake electrons in the $Z \to e^+e^-$ sample is estimated from data, as described in Sect. 6.2.1. The uncertainty on this background is 0.1% of the total Z yield. The expected background to $Z \to \mu^+\mu^-$ is 0.5%, with an uncertainty of 0.2%. Further uncertainty arises from the fit model of the backgrounds in subsamples where one of the muon candidates fails the selection. We estimate this uncertainty to be 1%. Uncertainties from the normalization of electroweak and $t\bar{t}$ backgrounds are negligible in both W and Z channels.

Theoretical uncertainties in the $W \to \ell\nu$ cross section measurement affect the estimation of the acceptance. The Monte Carlo estimates are based on simulations that use a next-to-leading order (NLO) generator (POWHEG) as input. Events are re-weighted at generator level according to different PDF set assumptions (CTEQ6.6 [22], MSTW08NLO [23], NNPDF2.0 [24]). The observed variations in the acceptance are less than 1.2%. Remaining theoretical uncertainties associated with the treatment of initial-state radiation, final-state QED radiation, missing electroweak effects, and renormalization and factorization scale assumptions amount to approximately 1.5%.

Table 1 shows a summary of the systematic uncertainties for the W and Z cross section measurements.

# 8 Results

All theoretical predictions quoted in this section are computed at the next-to-next-to-leading order (NNLO) with the program FEWZ [25, 26] and the MSTW08 set of PDFs. The uncertainties correspond to 68% confidence levels obtained by combining the PDF and $\alpha_S$ errors from the MSTW08, CTEQ6.6, and NNPDF2.0 groups and adding the NNLO scale uncertainties in quadrature, as prescribed by the PDF4LHC working group [27].

For all measurements we present results for electron and muon channels separately and, assuming lepton universality in W and Z decays, for the combined lepton channel. The electron and muon channels are combined by maximizing a likelihood that accounts for the individual statistical and systematic uncertainties and their correlations. For cross section measurements, correlations are only numerically relevant for theoretical uncertainties, including the PDF uncertainties on the acceptance values. For cross section ratio measurements, the correlations of lepton efficiencies are taken into account in each lepton channel, with other experimental uncertainties assumed uncorrelated; in the combination of lepton channels, we assume fully-correlated uncertainty for the acceptance factor, with other uncertainties assumed uncorrelated.

Table 2: Summary of production cross section times branching ratio measurements and their theoretical predictions.

| Channel | | $\sigma \times \mathcal{B}$ (nb) | NNLO (nb) |
|---|---|---|---|
| W | $e\nu$ | $10.04 \pm 0.10\,(\text{stat.}) \pm 0.52\,(\text{syst.}) \pm 1.10\,(\text{lumi.})$ | $10.44 \pm 0.52$ |
| | $\mu\nu$ | $9.92 \pm 0.09\,(\text{stat.}) \pm 0.31\,(\text{syst.}) \pm 1.09\,(\text{lumi.})$ | |
| | $\ell\nu$ | $9.95 \pm 0.07\,(\text{stat.}) \pm 0.28\,(\text{syst.}) \pm 1.09\,(\text{lumi.})$ | |
| $W^+$ | $e^+\nu$ | $5.93 \pm 0.07\,(\text{stat.}) \pm 0.36\,(\text{syst.}) \pm 0.65\,(\text{lumi.})$ | $6.15 \pm 0.29$ |
| | $\mu^+\nu$ | $5.84 \pm 0.07\,(\text{stat.}) \pm 0.18\,(\text{syst.}) \pm 0.64\,(\text{lumi.})$ | |
| | $\ell^+\nu$ | $5.86 \pm 0.06\,(\text{stat.}) \pm 0.17\,(\text{syst.}) \pm 0.64\,(\text{lumi.})$ | |
| $W^-$ | $e^-\bar{\nu}$ | $4.14 \pm 0.06\,(\text{stat.}) \pm 0.25\,(\text{syst.}) \pm 0.45\,(\text{lumi.})$ | $4.29 \pm 0.23$ |
| | $\mu^-\bar{\nu}$ | $4.08 \pm 0.06\,(\text{stat.}) \pm 0.15\,(\text{syst.}) \pm 0.45\,(\text{lumi.})$ | |
| | $\ell^-\bar{\nu}$ | $4.09 \pm 0.05\,(\text{stat.}) \pm 0.14\,(\text{syst.}) \pm 0.45\,(\text{lumi.})$ | |
| Z | $e^+e^-$ | $0.960 \pm 0.037\,(\text{stat.}) \pm 0.059\,(\text{syst.}) \pm 0.106\,(\text{lumi.})$ | $0.972 \pm 0.042$ |
| | $\mu^+\mu^-$ | $0.924 \pm 0.031\,(\text{stat.}) \pm 0.022\,(\text{syst.}) \pm 0.102\,(\text{lumi.})$ | |
| | $\ell^+\ell^-$ | $0.931 \pm 0.026\,(\text{stat.}) \pm 0.023\,(\text{syst.}) \pm 0.102\,(\text{lumi.})$ | |

The measured cross sections times branching ratio for W, $W^+$, $W^-$ and Z production are reported in Table 2, for the electron, muon, and combined lepton ($\ell$ = e or $\mu$) channels, along with predictions at the NNLO in QCD. The reported Z boson production cross sections pertain to the invariant mass range $60 < M_{\ell^+\ell^-} < 120$ GeV, and are corrected for the fiducial and kinematic acceptance but not for $\gamma^*$ exchange.

The ratio of cross sections for W and Z production is

$$R_{W/Z} = \frac{[\sigma \times \mathcal{B}](W)}{[\sigma \times \mathcal{B}](Z)} = \frac{N_W}{N_Z}\frac{\rho_Z}{\rho_W}\frac{F_Z}{F_W} = \frac{N_W}{N_Z}\frac{\varepsilon_Z}{\varepsilon_W}\frac{A_Z}{A_W},$$

where $A_W$ and $A_Z$ are the fiducial and kinematic acceptances for $W \to \ell\nu$ and $Z \to \ell^+\ell^-$, respectively, and $\varepsilon_W$ and $\varepsilon_Z$ are the selection efficiencies for W and Z signal events in the acceptance. The uncertainty from $A_W/A_Z$ is determined from Monte Carlo generator studies to be approximately 1%.

The ratio of cross sections for $W^+$ and $W^-$ production is

$$R_{+/-} = \frac{[\sigma \times \mathcal{B}](W^+)}{[\sigma \times \mathcal{B}](W^-)} = \frac{N_{W^+}}{N_{W^-}} \frac{\rho_{W^-}}{\rho_{W^+}} \frac{F_{W^-}}{F_{W^+}} = \frac{N_{W^+}}{N_{W^-}} \frac{\varepsilon_{W^-}}{\varepsilon_{W^+}} \frac{A_{W^-}}{A_{W^+}},$$

where $A_{W^+}$ and $A_{W^-}$ are the fiducial and kinematic acceptances for $W^+ \to \ell^+\nu$ and $W^- \to \ell^-\overline{\nu}$, respectively, and $\varepsilon_{W^+}$ and $\varepsilon_{W^+}$ are the selection efficiencies for $W^+$ and $W^-$ signal events in the acceptance. The uncertainty from $A_{W^+}/A_{W^-}$ is determined from Monte Carlo generator studies to be approximately 2%.

Table 3: Summary of the cross section ratio measurements and their theoretical predictions.

| Quantity | | Ratio | NNLO |
|---|---|---|---|
| $R_{W/Z}$ | e | $10.47 \pm 0.42\,(\text{stat.}) \pm 0.47\,(\text{syst.})$ | $10.74 \pm 0.04$ |
| | $\mu$ | $10.74 \pm 0.37\,(\text{stat.}) \pm 0.33\,(\text{syst.})$ | |
| | $\ell$ | $10.64 \pm 0.28\,(\text{stat.}) \pm 0.29\,(\text{syst.})$ | |
| $R_{+/-}$ | e | $1.434 \pm 0.028\,(\text{stat.}) \pm 0.082\,(\text{syst.})$ | $1.435 \pm 0.044$ |
| | $\mu$ | $1.433 \pm 0.026\,(\text{stat.}) \pm 0.054\,(\text{syst.})$ | |
| | $\ell$ | $1.433 \pm 0.020\,(\text{stat.}) \pm 0.050\,(\text{syst.})$ | |

The measurements of the $R_{W/Z}$ and $R_{+/-}$ cross section ratios are reported in Table 3, along with their theoretical predictions.

We also report the cross sections as measured within the fiducial and kinematic acceptance, thereby eliminating the PDF uncertainties from the results. In effect, these uncertainties are transferred to the theoretical predictions, allowing for a cleaner separation of experimental and theoretical uncertainties. For each channel the fiducial and kinematic acceptance is defined by the fraction of events with lepton $p_T$ greater than 20 GeV after final-state QED radiation, and with pseudorapidity in the range $|\eta| < 2.5$ for electrons and $|\eta| < 2.1$ for muons.

Table 4: Summary of production cross section measurements in restricted fiducial and kinematic acceptances. The $p_T$ and $|\eta|$ criteria restricting the acceptance for electrons and muons, and the resulting acceptance values, are also given.

| Channel | $\sigma \times \mathcal{B}$ in acceptance $A$ (nb) | $A$ | |
|---|---|---|---|
| $W \to e\nu_e$ | $6.04 \pm 0.06\,(\text{stat.}) \pm 0.31\,(\text{syst.}) \pm 0.66\,(\text{lumi.})$ | $0.601 \pm 0.005$ | $p_T > 20\,\text{GeV}$ $\lvert\eta\rvert < 2.5$ |
| $W^+ \to e^+\nu_e$ | $3.69 \pm 0.05\,(\text{stat.}) \pm 0.22\,(\text{syst.}) \pm 0.41\,(\text{lumi.})$ | $0.622 \pm 0.006$ | |
| $W^- \to e^-\overline{\nu}_e$ | $2.36 \pm 0.04\,(\text{stat.}) \pm 0.14\,(\text{syst.}) \pm 0.26\,(\text{lumi.})$ | $0.571 \pm 0.009$ | |
| $Z \to e^+e^-$ | $0.460 \pm 0.018\,(\text{stat.}) \pm 0.028\,(\text{syst.}) \pm 0.051\,(\text{lumi.})$ | $0.479 \pm 0.005$ | |
| $W \to \mu\nu_\mu$ | $5.21 \pm 0.05\,(\text{stat.}) \pm 0.15\,(\text{syst.}) \pm 0.57\,(\text{lumi.})$ | $0.525 \pm 0.006$ | $p_T > 20\,\text{GeV}$ $\lvert\eta\rvert < 2.1$ |
| $W^+ \to \mu^+\nu_\mu$ | $3.16 \pm 0.04\,(\text{stat.}) \pm 0.10\,(\text{syst.}) \pm 0.35\,(\text{lumi.})$ | $0.541 \pm 0.006$ | |
| $W^- \to \mu^-\overline{\nu}_\mu$ | $2.05 \pm 0.03\,(\text{stat.}) \pm 0.06\,(\text{syst.}) \pm 0.22\,(\text{lumi.})$ | $0.502 \pm 0.006$ | |
| $Z \to \mu^+\mu^-$ | $0.368 \pm 0.012\,(\text{stat.}) \pm 0.007\,(\text{syst.}) \pm 0.040\,(\text{lumi.})$ | $0.398 \pm 0.005$ | |

The measurements of cross sections in restricted acceptance regions are reported in Table 4, along with the acceptance values, computed using the POWHEG generator, which is complete to the NLO and interfaced with PYTHIA for final-state radiation (FSR). Acceptance values from FEWZ, which is complete to the NNLO but lacks FSR, are compatible with those from

Table 5: The ratios of the W and Z cross section times branching ratio measurements to their theoretical predictions, and of the measured cross section ratios to their theoretical predictions. The uncertainty in the integrated luminosity cancels out in the latter ratios.

| Quantity | | Ratio (CMS/Theory) | Lumi. Uncertainty |
|---|---|---|---|
| $\sigma \times \mathcal{B}$ | W | $0.953 \pm 0.028\,(\text{exp.}) \pm 0.048\,(\text{theo.})$ | $\pm 0.11$ |
| | $W^+$ | $0.953 \pm 0.029\,(\text{exp.}) \pm 0.045\,(\text{theo.})$ | |
| | $W^-$ | $0.954 \pm 0.034\,(\text{exp.}) \pm 0.051\,(\text{theo.})$ | |
| | Z | $0.960 \pm 0.036\,(\text{exp.}) \pm 0.040\,(\text{theo.})$ | |
| $R_{W/Z}$ | | $0.990 \pm 0.038\,(\text{exp.}) \pm 0.004\,(\text{theo.})$ | nil |
| $R_{+/-}$ | | $1.002 \pm 0.038\,(\text{exp.}) \pm 0.028\,(\text{theo.})$ | |

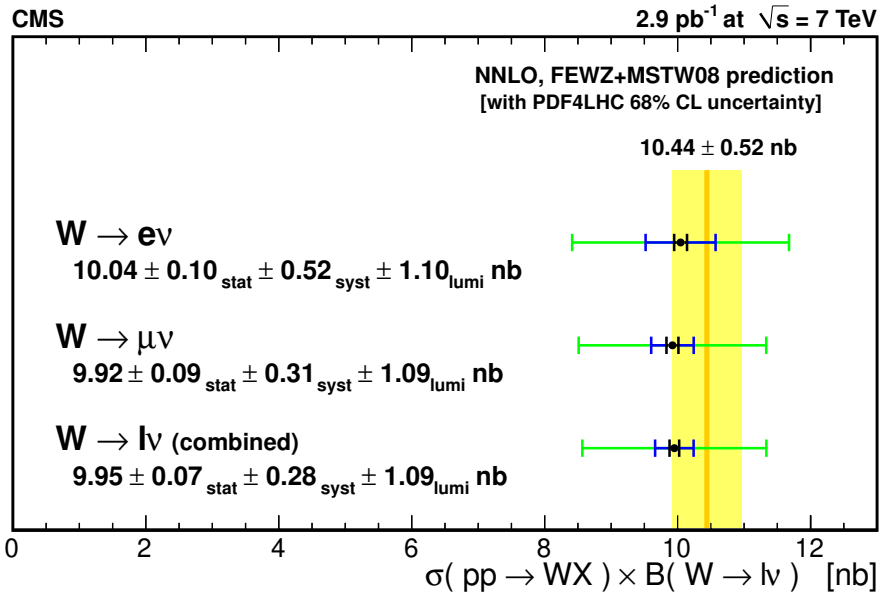


Figure 3: Summary of the W boson production cross section times branching ratio measurements.

POWHEG. The quoted errors on the acceptances are due to the PDF uncertainties. Since the acceptances are different for electrons and muons, these cross section values cannot be combined. The difference in acceptance for $W^+$ and $W^-$, larger in the electron channel, is a consequence of the pseudorapidity distributions of $\ell^+$ and $\ell^-$ from boson decays, which reflect not only the different $x$ distributions of quarks and antiquarks in the proton, but also a distinction between valence and sea quarks at a given $x$ due to the V–A interaction.

Summaries of the measurements are given in Figs. 3, 4, 5, and 6, illustrating the consistency of the measurements in the electron and muon channels, as well as the confirmation of theoretical predictions computed at the NNLO in QCD with state-of-the-art PDF sets. For each reported measurement, the statistical error is represented in black and the total experimental uncertainty, obtained by adding in quadrature the statistical and systematic uncertainties, in dark blue. For the cross section measurements, the luminosity uncertainty is added linearly to the experimental uncertainty, and is represented in green. The dark-yellow vertical line represents the theoretical prediction, and the light-yellow vertical band is the theoretical uncertainty,

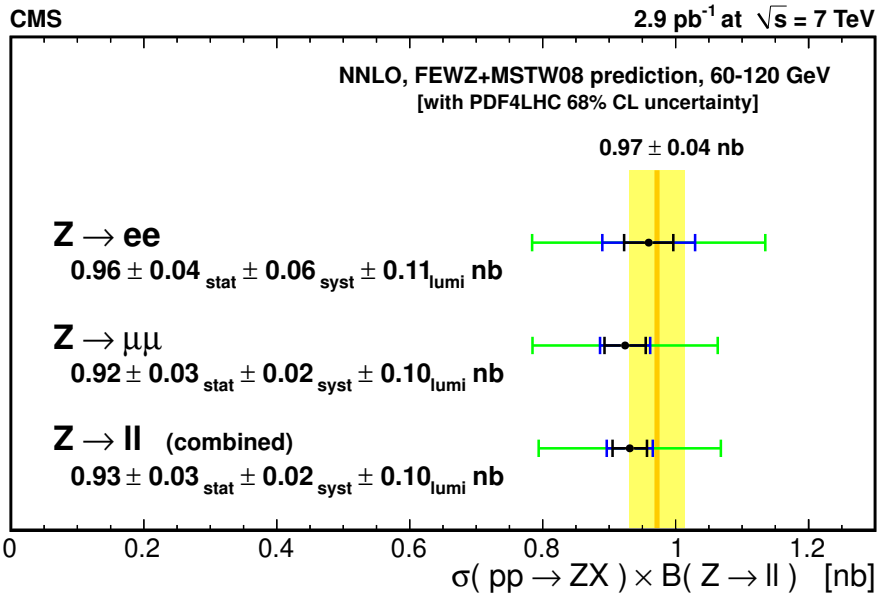


Figure 4: Summary of the Z boson production cross section times branching ratio measurements.

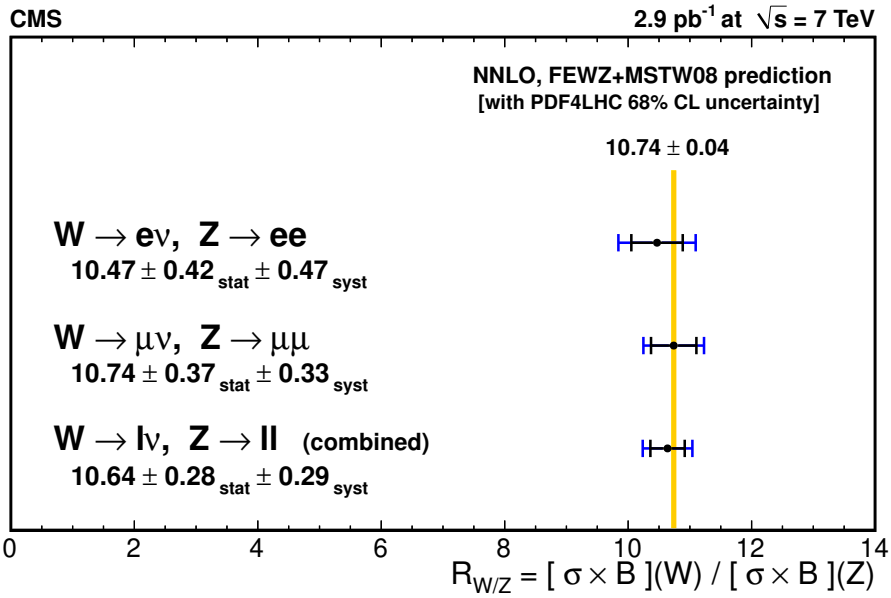


Figure 5: Summary of the $R_{W/Z}$ cross section ratio measurements.

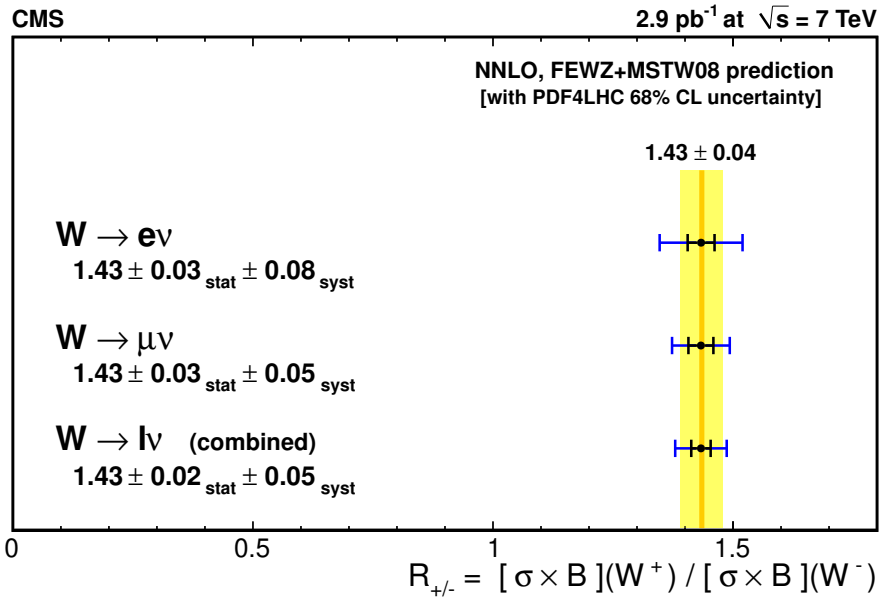


Figure 6: Summary of the $R_{+/-}$ cross section ratio measurements.

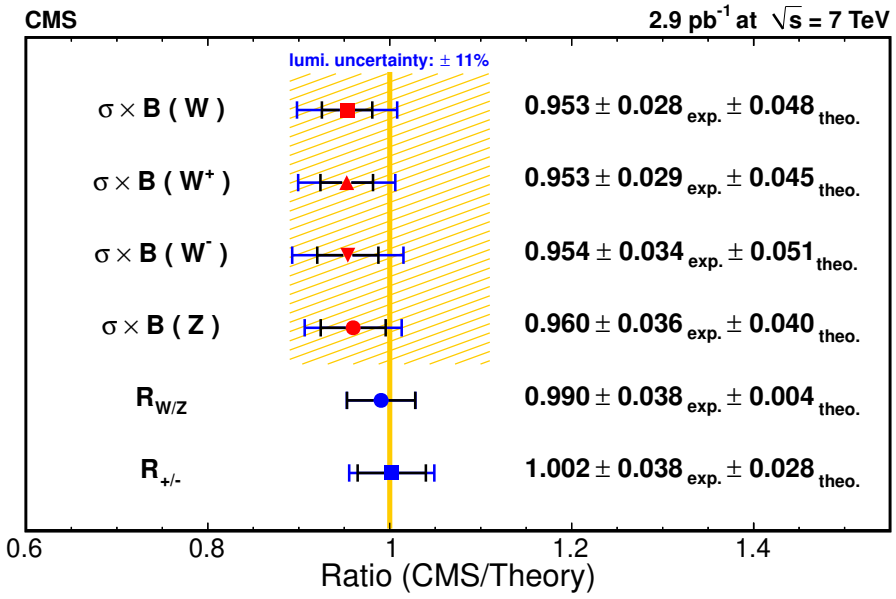


Figure 7: Summary of the ratios of the CMS measurements to their theoretical predictions. The luminosity uncertainty (±11%), which affects only the cross section times branching ratio measurements, is represented by a shaded area.

interpreted as a 68% confidence interval, as described above.

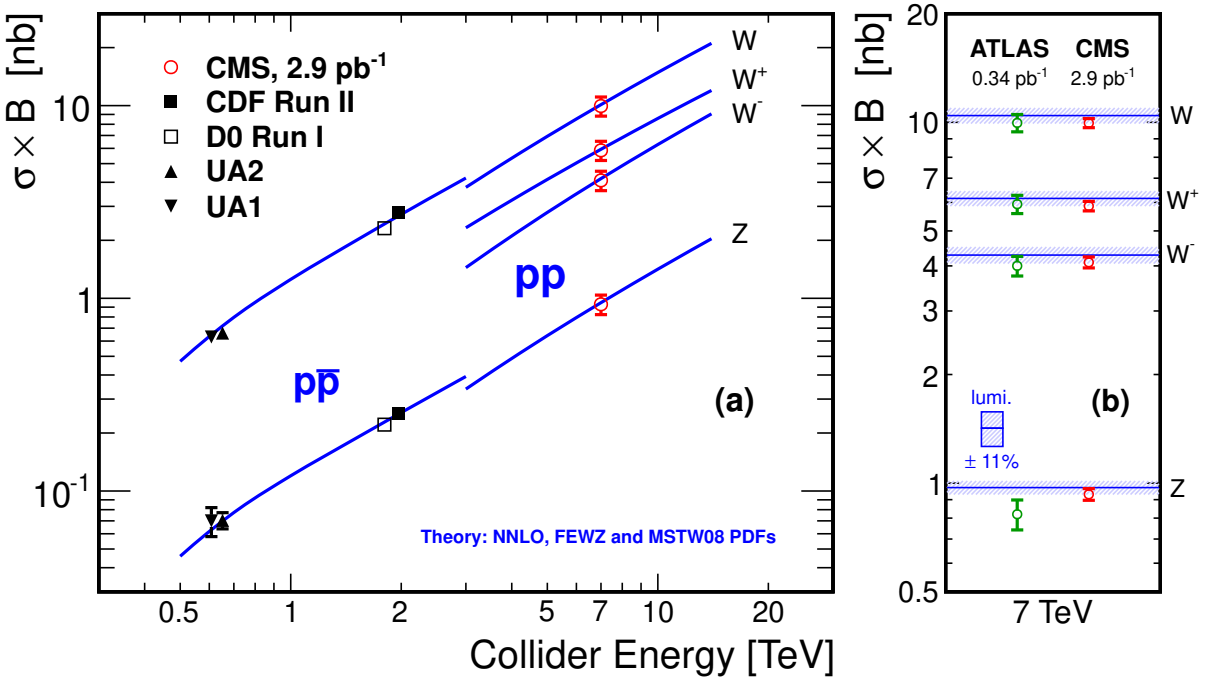


Figure 8: (a) Measurements of inclusive W and Z production cross sections times branching ratio as a function of center-of-mass energy for CMS and experiments at lower-energy colliders. The lines are the NNLO theory predictions. (b) Comparison of the ATLAS and CMS W and Z production cross sections times branching ratios. The error bars are the statistical and systematic uncertainties added in quadrature, except for the uncertainty on the integrated luminosity, whose value is shown separately as a band.

The agreement of theoretical predictions with our measurements is quantified in Table 5 and illustrated in Fig. 7. There, the experimental uncertainty ("exp") is computed as the sum in quadrature of the statistical uncertainty and the systematic uncertainties aside from the theoretical uncertainties associated with the acceptance. The theoretical uncertainty ("theo") is computed by adding in quadrature the variations of the central value when the renormalization scale is varied, and the PDF uncertainty. Figure 8 (a) represents the CMS measurements together with measurements at lower-energy hadron colliders. The increase of the W and Z cross sections with energy is confirmed. Fig. 8 (b) shows the good agreement between CMS and ATLAS measurements in pp collisions at $\sqrt{s} = 7$ TeV.

## 9 Conclusions

We have performed measurements of inclusive W and Z boson production cross sections in pp collisions at $\sqrt{s} = 7$ TeV using $(2.88 \pm 0.32)$ pb$^{-1}$ of data recorded by the CMS detector at the LHC. We find internal consistency between measurements in the electron and muon channels and report their combination. We also report ratios of W to Z and $W^+$ to $W^-$ production cross sections. The theoretical predictions agree with our measurements, as illustrated in Fig. 7.

Aside from the luminosity uncertainty, which cancels in the ratios, the systematic uncertainties are comparable to the statistical ones in our measurements. The experimental uncertainties are smaller than those on the theoretical predictions; they are typically less than 4%. This suggests

that the inclusive measurements of W and Z cross sections can potentially be used to normalize the LHC luminosity at the 5% level or better [28]. As most of the systematic uncertainties are statistical in nature, they will decrease with larger data samples, and also benefit from an improved understanding of the CMS detector.

## References


[1] UA1 Collaboration, "Studies of Intermediate Vector Boson Production and Decay in UA1 at the CERN Proton - Antiproton Collider", *Z. Phys.* **C44** (1989) 15. doi:10.1007/BF01548582.

[2] UA2 Collaboration, "Measurement of W and Z Production Cross Sections at the CERN $\overline{\mathrm{p}}\mathrm{p}$ Collider", *Z. Phys.* **C47** (1990) 11. doi:10.1007/BF01551906.

[3] CDF Collaboration, "First measurements of inclusive W and Z cross sections from Run II of the Tevatron collider", *Phys. Rev. Lett.* **94** (2005) 091803, arXiv:hep-ex/0406078. doi:10.1103/PhysRevLett.94.091803.

[4] CDF Collaboration, "The transverse momentum and total cross section of $\mathrm{e}^+\mathrm{e}^-$ pairs in the Z boson region from $\mathrm{p}\overline{\mathrm{p}}$ collisions at $\sqrt{s} = 1.8$ TeV", *Phys. Rev. Lett.* **84** (2000) 845, arXiv:hep-ex/0001021. doi:10.1103/PhysRevLett.84.845.

[5] D0 Collaboration, "Extraction of the width of the W boson from measurements of $\sigma(\mathrm{p}\overline{\mathrm{p}} \to \mathrm{W} + X) \times \mathcal{B}(\mathrm{W} \to \mathrm{e}\nu)$ and $\sigma(\mathrm{p}\overline{\mathrm{p}} \to \mathrm{Z} + X) \times \mathcal{B}(\mathrm{Z} \to \mathrm{e}^+\mathrm{e}^-)$ and their ratio", *Phys. Rev.* **D61** (2000) 072001, arXiv:hep-ex/9906025. doi:10.1103/PhysRevD.61.072001.

[6] ATLAS Collaboration, "Measurement of the $\mathrm{W} \to \ell\nu$ and $\mathrm{Z}/\gamma^* \to \ell^+\ell^-$ production cross sections in proton-proton collisions at $\sqrt{s} = 7$ TeV with the ATLAS detector", arXiv:1010.2130.

[7] CMS Collaboration, "The CMS experiment at the CERN LHC", *JINST* **0803** (2008) S08004.

[8] CMS Collaboration, "The CMS High Level Trigger", *Eur. Phys. J.* **C46** (2006) 605.

[9] CMS Collaboration, "Electromagnetic calorimeter calibration with 7 TeV data", *CMS Physics Analysis Summary* **CMS-PAS-EGM-10-003** (2010).

[10] CMS Collaboration, "Reconstruction of Electrons with the Gaussian-Sum Filter in the CMS Tracker at the LHC", *CMS Note* **CMS-2005/001** (2005).

[11] CMS Collaboration, "Electron Reconstruction and Selection Studies with First CMS 7 TeV Data", *CMS Physics Analysis Summary* **CMS-PAS-EGM-10-004** (2010).

[12] CMS Collaboration, "Performance of muon identification in pp collisions at $\sqrt{s}$ = 7 TeV", *CMS Physics Analysis Summary* **CMS-PAS-MUO-10-002** (2010).

[13] CMS Collaboration, "Commissioning of the particle-flow event reconstruction with leptons from J/$\Psi$ and W decays at 7 TeV", *CMS Physics Analysis Summary* **CMS-PAS-PFT-10-003** (2010).

[14] CMS Collaboration, "CMS MET Performance in Events Containing Electroweak Bosons from pp Collisions at $\sqrt{s} = 7$ TeV", *CMS Physics Analysis Summary* **CMS-PAS-JME-10-005** (2010).

[15] S. Alioli et al., "NLO vector-boson production matched with shower in POWHEG", *JHEP* **07** (2008) 060, arXiv:0805.4802. doi:10.1088/1126-6708/2008/07/060.

[16] P. Nason, "A new method for combining NLO QCD with shower Monte Carlo algorithms", *JHEP* **11** (2004) 040, arXiv:hep-ph/0409146. doi:10.1088/1126-6708/2004/11/040.

[17] S. Frixione, P. Nason, and C. Oleari, "Matching NLO QCD computations with Parton Shower simulations: the POWHEG method", *JHEP* **11** (2007) 070, arXiv:0709.2092. doi:10.1088/1126-6708/2007/11/070.

[18] T. Sjöstrand, S. Mrenna, and P.Z. Skands, "PYTHIA 6.4 Physics and Manual", *JHEP* **05** (2006) 026, arXiv:hep-ph/0603175.

[19] S. Agostinelli et al., "GEANT4: A simulation toolkit", *Nucl. Instrum. Meth.* **A506** (2003) 250. doi:10.1016/S0168-9002(03)01368-8.

[20] CMS Collaboration, "Measurement of the charge ratio of atmospheric muons with the CMS detector", *Phys. Lett.* **B692** (2010) 83.

[21] CMS Collaboration, "Measurement of CMS Luminosity", *CMS Physics Analysis Summary* **CMS-PAS-EWK-10-004** (2010).

[22] P. M. Nadolsky et al., "Implications of CTEQ global analysis for collider observables", *Phys. Rev.* **D78** (2008) 013004, arXiv:0802.0007. doi:10.1103/PhysRevD.78.013004.

[23] A. D. Martin et al., "Parton distributions for the LHC", *Eur. Phys. J.* **C63** (2009) 189, arXiv:0901.0002. doi:10.1140/epjc/s10052-009-1072-5.

[24] R. D. Ball et al., "A first unbiased global NLO determination of parton distributions and their uncertainties", arXiv:1002.4407.

[25] K. Melnikov and F. Petriello, "Electroweak gauge boson production at hadron colliders through $\mathcal{O}(\alpha_s^2)$", *Phys. Rev.* **D74** (2006) 114017, arXiv:hep-ph/0609070. doi:10.1103/PhysRevD.74.114017.

[26] K. Melnikov and F. Petriello, "The W boson production cross section at the LHC through $\mathcal{O}(\alpha_s^2)$", *Phys. Rev. Lett.* **96** (2006) 231803, arXiv:hep-ph/0603182. doi:10.1103/PhysRevLett.96.231803.

[27] The PDF4LHC Working Group, "Recommendation for LHC cross section calculations". http://www.hep.ucl.ac.uk/pdf4lhc/.

[28] M. Dittmar, F. Pauss, and D. Zurcher, "Towards a precise parton luminosity determination at the CERN LHC", *Phys. Rev.* **D56** (1997) 7284, arXiv:hep-ex/9705004. doi:10.1103/PhysRevD.56.7284.

# A The CMS Collaboration

**Yerevan Physics Institute, Yerevan, Armenia**
V. Khachatryan, A.M. Sirunyan, A. Tumasyan

**Institut für Hochenergiephysik der OeAW, Wien, Austria**
W. Adam, T. Bergauer, M. Dragicevic, J. Erö, C. Fabjan, M. Friedl, R. Frühwirth, V.M. Ghete, J. Hammer[1], S. Hänsel, C. Hartl, M. Hoch, N. Hörmann, J. Hrubec, M. Jeitler, G. Kasieczka, W. Kiesenhofer, M. Krammer, D. Liko, I. Mikulec, M. Pernicka, H. Rohringer, R. Schöfbeck, J. Strauss, A. Taurok, F. Teischinger, W. Waltenberger, G. Walzel, E. Widl, C.-E. Wulz

**National Centre for Particle and High Energy Physics, Minsk, Belarus**
V. Mossolov, N. Shumeiko, J. Suarez Gonzalez

**Universiteit Antwerpen, Antwerpen, Belgium**
L. Benucci, L. Ceard, K. Cerny, E.A. De Wolf, X. Janssen, T. Maes, L. Mucibello, S. Ochesanu, B. Roland, R. Rougny, M. Selvaggi, H. Van Haevermaet, P. Van Mechelen, N. Van Remortel

**Vrije Universiteit Brussel, Brussel, Belgium**
V. Adler, S. Beauceron, F. Blekman, S. Blyweert, J. D'Hondt, O. Devroede, R. Gonzalez Suarez, A. Kalogeropoulos, J. Maes, M. Maes, S. Tavernier, W. Van Doninck, P. Van Mulders, G.P. Van Onsem, I. Villella

**Université Libre de Bruxelles, Bruxelles, Belgium**
O. Charaf, B. Clerbaux, G. De Lentdecker, V. Dero, A.P.R. Gay, G.H. Hammad, T. Hreus, P.E. Marage, L. Thomas, C. Vander Velde, P. Vanlaer, J. Wickens

**Ghent University, Ghent, Belgium**
S. Costantini, M. Grunewald, B. Klein, A. Marinov, J. Mccartin, D. Ryckbosch, F. Thyssen, M. Tytgat, L. Vanelderen, P. Verwilligen, S. Walsh, N. Zaganidis

**Université Catholique de Louvain, Louvain-la-Neuve, Belgium**
S. Basegmez, G. Bruno, J. Caudron, J. De Favereau De Jeneret, C. Delaere, P. Demin, D. Favart, A. Giammanco, G. Grégoire, J. Hollar, V. Lemaitre, J. Liao, O. Militaru, S. Ovyn, D. Pagano, A. Pin, K. Piotrzkowski, L. Quertenmont, N. Schul

**Université de Mons, Mons, Belgium**
N. Beliy, T. Caebergs, E. Daubie

**Centro Brasileiro de Pesquisas Fisicas, Rio de Janeiro, Brazil**
G.A. Alves, D. De Jesus Damiao, M.E. Pol, M.H.G. Souza

**Universidade do Estado do Rio de Janeiro, Rio de Janeiro, Brazil**
W. Carvalho, E.M. Da Costa, C. De Oliveira Martins, S. Fonseca De Souza, L. Mundim, H. Nogima, V. Oguri, W.L. Prado Da Silva, A. Santoro, S.M. Silva Do Amaral, A. Sznajder, F. Torres Da Silva De Araujo

**Instituto de Fisica Teorica, Universidade Estadual Paulista, Sao Paulo, Brazil**
F.A. Dias, M.A.F. Dias, T.R. Fernandez Perez Tomei, E. M. Gregores[2], F. Marinho, S.F. Novaes, Sandra S. Padula

**Institute for Nuclear Research and Nuclear Energy, Sofia, Bulgaria**
N. Darmenov[1], L. Dimitrov, V. Genchev[1], P. Iaydjiev[1], S. Piperov, M. Rodozov, S. Stoykova, G. Sultanov, V. Tcholakov, R. Trayanov, I. Vankov

**University of Sofia, Sofia, Bulgaria**
M. Dyulendarova, R. Hadjiiska, V. Kozhuharov, L. Litov, E. Marinova, M. Mateev, B. Pavlov, P. Petkov

**Institute of High Energy Physics, Beijing, China**
J.G. Bian, G.M. Chen, H.S. Chen, C.H. Jiang, D. Liang, S. Liang, J. Wang, J. Wang, X. Wang, Z. Wang, M. Xu, M. Yang, J. Zang, Z. Zhang

**State Key Lab. of Nucl. Phys. and Tech., Peking University, Beijing, China**
Y. Ban, S. Guo, W. Li, Y. Mao, S.J. Qian, H. Teng, B. Zhu

**Universidad de Los Andes, Bogota, Colombia**
A. Cabrera, B. Gomez Moreno, A.A. Ocampo Rios, A.F. Osorio Oliveros, J.C. Sanabria

**Technical University of Split, Split, Croatia**
N. Godinovic, D. Lelas, K. Lelas, R. Plestina[3], D. Polic, I. Puljak

**University of Split, Split, Croatia**
Z. Antunovic, M. Dzelalija

**Institute Rudjer Boskovic, Zagreb, Croatia**
V. Brigljevic, S. Duric, K. Kadija, S. Morovic

**University of Cyprus, Nicosia, Cyprus**
A. Attikis, M. Galanti, J. Mousa, C. Nicolaou, F. Ptochos, P.A. Razis, H. Rykaczewski

**Academy of Scientific Research and Technology of the Arab Republic of Egypt, Egyptian Network of High Energy Physics, Cairo, Egypt**
Y. Assran[4], M.A. Mahmoud[5]

**National Institute of Chemical Physics and Biophysics, Tallinn, Estonia**
A. Hektor, M. Kadastik, K. Kannike, M. Müntel, M. Raidal, L. Rebane

**Department of Physics, University of Helsinki, Helsinki, Finland**
V. Azzolini, P. Eerola

**Helsinki Institute of Physics, Helsinki, Finland**
S. Czellar, J. Härkönen, A. Heikkinen, V. Karimäki, R. Kinnunen, J. Klem, M.J. Kortelainen, T. Lampén, K. Lassila-Perini, S. Lehti, T. Lindén, P. Luukka, T. Mäenpää, E. Tuominen, J. Tuominiemi, E. Tuovinen, D. Ungaro, L. Wendland

**Lappeenranta University of Technology, Lappeenranta, Finland**
K. Banzuzi, A. Korpela, T. Tuuva

**Laboratoire d'Annecy-le-Vieux de Physique des Particules, IN2P3-CNRS, Annecy-le-Vieux, France**
D. Sillou

**DSM/IRFU, CEA/Saclay, Gif-sur-Yvette, France**
M. Besancon, M. Dejardin, D. Denegri, B. Fabbro, J.L. Faure, F. Ferri, S. Ganjour, F.X. Gentit, A. Givernaud, P. Gras, G. Hamel de Monchenault, P. Jarry, E. Locci, J. Malcles, M. Marionneau, L. Millischer, J. Rander, A. Rosowsky, I. Shreyber, M. Titov, P. Verrecchia

**Laboratoire Leprince-Ringuet, Ecole Polytechnique, IN2P3-CNRS, Palaiseau, France**
S. Baffioni, F. Beaudette, L. Bianchini, M. Bluj[6], C. Broutin, P. Busson, C. Charlot, T. Dahms, L. Dobrzynski, R. Granier de Cassagnac, M. Haguenauer, P. Miné, C. Mironov, C. Ochando, P. Paganini, D. Sabes, R. Salerno, Y. Sirois, C. Thiebaux, B. Wyslouch[7], A. Zabi

**Institut Pluridisciplinaire Hubert Curien, Université de Strasbourg, Université de Haute Alsace Mulhouse, CNRS/IN2P3, Strasbourg, France**
J.-L. Agram[8], J. Andrea, A. Besson, D. Bloch, D. Bodin, J.-M. Brom, M. Cardaci, E.C. Chabert, C. Collard, E. Conte[8], F. Drouhin[8], C. Ferro, J.-C. Fontaine[8], D. Gelé, U. Goerlach, S. Greder, P. Juillot, M. Karim[8], A.-C. Le Bihan, Y. Mikami, P. Van Hove

**Centre de Calcul de l'Institut National de Physique Nucleaire et de Physique des Particules (IN2P3), Villeurbanne, France**
F. Fassi, D. Mercier

**Université de Lyon, Université Claude Bernard Lyon 1, CNRS-IN2P3, Institut de Physique Nucléaire de Lyon, Villeurbanne, France**
C. Baty, N. Beaupere, M. Bedjidian, O. Bondu, G. Boudoul, D. Boumediene, H. Brun, N. Chanon, R. Chierici, D. Contardo, P. Depasse, H. El Mamouni, A. Falkiewicz, J. Fay, S. Gascon, B. Ille, T. Kurca, T. Le Grand, M. Lethuillier, L. Mirabito, S. Perries, V. Sordini, S. Tosi, Y. Tschudi, P. Verdier, H. Xiao

**E. Andronikashvili Institute of Physics, Academy of Science, Tbilisi, Georgia**
V. Roinishvili

**RWTH Aachen University, I. Physikalisches Institut, Aachen, Germany**
G. Anagnostou, M. Edelhoff, L. Feld, N. Heracleous, O. Hindrichs, R. Jussen, K. Klein, J. Merz, N. Mohr, A. Ostapchuk, A. Perieanu, F. Raupach, J. Sammet, S. Schael, D. Sprenger, H. Weber, M. Weber, B. Wittmer

**RWTH Aachen University, III. Physikalisches Institut A, Aachen, Germany**
M. Ata, W. Bender, M. Erdmann, J. Frangenheim, T. Hebbeker, A. Hinzmann, K. Hoepfner, C. Hof, T. Klimkovich, D. Klingebiel, P. Kreuzer, D. Lanske†, C. Magass, G. Masetti, M. Merschmeyer, A. Meyer, P. Papacz, H. Pieta, H. Reithler, S.A. Schmitz, L. Sonnenschein, J. Steggemann, D. Teyssier

**RWTH Aachen University, III. Physikalisches Institut B, Aachen, Germany**
M. Bontenackels, M. Davids, M. Duda, G. Flügge, H. Geenen, M. Giffels, W. Haj Ahmad, D. Heydhausen, T. Kress, Y. Kuessel, A. Linn, A. Nowack, L. Perchalla, O. Pooth, J. Rennefeld, P. Sauerland, A. Stahl, M. Thomas, D. Tornier, M.H. Zoeller

**Deutsches Elektronen-Synchrotron, Hamburg, Germany**
M. Aldaya Martin, W. Behrenhoff, U. Behrens, M. Bergholz[9], K. Borras, A. Cakir, A. Campbell, E. Castro, D. Dammann, G. Eckerlin, D. Eckstein, A. Flossdorf, G. Flucke, A. Geiser, I. Glushkov, J. Hauk, H. Jung, M. Kasemann, I. Katkov, P. Katsas, C. Kleinwort, H. Kluge, A. Knutsson, D. Krücker, E. Kuznetsova, W. Lange, W. Lohmann[9], R. Mankel, M. Marienfeld, I.-A. Melzer-Pellmann, A.B. Meyer, J. Mnich, A. Mussgiller, J. Olzem, A. Parenti, A. Raspereza, A. Raval, R. Schmidt[9], T. Schoerner-Sadenius, N. Sen, M. Stein, J. Tomaszewska, D. Volyanskyy, R. Walsh, C. Wissing

**University of Hamburg, Hamburg, Germany**
C. Autermann, S. Bobrovskyi, J. Draeger, H. Enderle, U. Gebbert, K. Kaschube, G. Kaussen, R. Klanner, J. Lange, B. Mura, S. Naumann-Emme, F. Nowak, N. Pietsch, C. Sander, H. Schettler, P. Schleper, M. Schröder, T. Schum, J. Schwandt, A.K. Srivastava, H. Stadie, G. Steinbrück, J. Thomsen, R. Wolf

**Institut für Experimentelle Kernphysik, Karlsruhe, Germany**
J. Bauer, V. Buege, T. Chwalek, W. De Boer, A. Dierlamm, G. Dirkes, M. Feindt, J. Gruschke, C. Hackstein, F. Hartmann, S.M. Heindl, M. Heinrich, H. Held, K.H. Hoffmann, S. Honc,

T. Kuhr, D. Martschei, S. Mueller, Th. Müller, M. Niegel, O. Oberst, A. Oehler, J. Ott, T. Peiffer, D. Piparo, G. Quast, K. Rabbertz, F. Ratnikov, M. Renz, C. Saout, A. Scheurer, P. Schieferdecker, F.-P. Schilling, G. Schott, H.J. Simonis, F.M. Stober, D. Troendle, J. Wagner-Kuhr, M. Zeise, V. Zhukov[10], E.B. Ziebarth

**Institute of Nuclear Physics "Demokritos", Aghia Paraskevi, Greece**
G. Daskalakis, T. Geralis, S. Kesisoglou, A. Kyriakis, D. Loukas, I. Manolakos, A. Markou, C. Markou, C. Mavrommatis, E. Petrakou

**University of Athens, Athens, Greece**
L. Gouskos, T.J. Mertzimekis, A. Panagiotou[1]

**University of Ioánnina, Ioánnina, Greece**
I. Evangelou, C. Foudas, P. Kokkas, N. Manthos, I. Papadopoulos, V. Patras, F.A. Triantis

**KFKI Research Institute for Particle and Nuclear Physics, Budapest, Hungary**
A. Aranyi, G. Bencze, L. Boldizsar, G. Debreczeni, C. Hajdu[1], D. Horvath[11], A. Kapusi, K. Krajczar[12], A. Laszlo, F. Sikler, G. Vesztergombi[12]

**Institute of Nuclear Research ATOMKI, Debrecen, Hungary**
N. Beni, J. Molnar, J. Palinkas, Z. Szillasi, V. Veszpremi

**University of Debrecen, Debrecen, Hungary**
P. Raics, Z.L. Trocsanyi, B. Ujvari

**Panjab University, Chandigarh, India**
S. Bansal, S.B. Beri, V. Bhatnagar, N. Dhingra, M. Jindal, M. Kaur, J.M. Kohli, M.Z. Mehta, N. Nishu, L.K. Saini, A. Sharma, A.P. Singh, J.B. Singh, S.P. Singh

**University of Delhi, Delhi, India**
S. Ahuja, S. Bhattacharya, B.C. Choudhary, P. Gupta, S. Jain, S. Jain, A. Kumar, R.K. Shivpuri

**Bhabha Atomic Research Centre, Mumbai, India**
R.K. Choudhury, D. Dutta, S. Kailas, S.K. Kataria, A.K. Mohanty[1], L.M. Pant, P. Shukla, P. Suggisetti

**Tata Institute of Fundamental Research - EHEP, Mumbai, India**
T. Aziz, M. Guchait[13], A. Gurtu, M. Maity[14], D. Majumder, G. Majumder, K. Mazumdar, G.B. Mohanty, A. Saha, K. Sudhakar, N. Wickramage

**Tata Institute of Fundamental Research - HECR, Mumbai, India**
S. Banerjee, S. Dugad, N.K. Mondal

**Institute for Studies in Theoretical Physics & Mathematics (IPM), Tehran, Iran**
H. Arfaei, H. Bakhshiansohi, S.M. Etesami, A. Fahim, M. Hashemi, A. Jafari, M. Khakzad, A. Mohammadi, M. Mohammadi Najafabadi, S. Paktinat Mehdiabadi, B. Safarzadeh, M. Zeinali

**INFN Sezione di Bari [a], Università di Bari [b], Politecnico di Bari [c], Bari, Italy**
M. Abbrescia[a,b], L. Barbone[a,b], C. Calabria[a,b], A. Colaleo[a], D. Creanza[a,c], N. De Filippis[a,c], M. De Palma[a,b], A. Dimitrov[a], L. Fiore[a], G. Iaselli[a,c], L. Lusito[a,b,1], G. Maggi[a,c], M. Maggi[a], N. Manna[a,b], B. Marangelli[a,b], S. My[a,c], S. Nuzzo[a,b], N. Pacifico[a,b], G.A. Pierro[a], A. Pompili[a,b], G. Pugliese[a,c], F. Romano[a,c], G. Roselli[a,b], G. Selvaggi[a,b], L. Silvestris[a], R. Trentadue[a], S. Tupputi[a,b], G. Zito[a]

**INFN Sezione di Bologna [a], Università di Bologna [b], Bologna, Italy**
G. Abbiendi[a], A.C. Benvenuti[a], D. Bonacorsi[a], S. Braibant-Giacomelli[a,b], P. Capiluppi[a,b], A. Castro[a,b], F.R. Cavallo[a], M. Cuffiani[a,b], G.M. Dallavalle[a], F. Fabbri[a], A. Fanfani[a,b], D. Fasanella[a], P. Giacomelli[a], M. Giunta[a], S. Marcellini[a], M. Meneghelli[a,b], A. Montanari[a], F.L. Navarria[a,b], F. Odorici[a], A. Perrotta[a], F. Primavera[a], A.M. Rossi[a,b], T. Rovelli[a,b], G. Siroli[a,b], R. Travaglini[a,b]

**INFN Sezione di Catania [a], Università di Catania [b], Catania, Italy**
S. Albergo[a,b], G. Cappello[a,b], M. Chiorboli[a,b,1], S. Costa[a,b], A. Tricomi[a,b], C. Tuve[a]

**INFN Sezione di Firenze [a], Università di Firenze [b], Firenze, Italy**
G. Barbagli[a], V. Ciulli[a,b], C. Civinini[a], R. D'Alessandro[a,b], E. Focardi[a,b], S. Frosali[a,b], E. Gallo[a], C. Genta[a], P. Lenzi[a,b], M. Meschini[a], S. Paoletti[a], G. Sguazzoni[a], A. Tropiano[a,1]

**INFN Laboratori Nazionali di Frascati, Frascati, Italy**
L. Benussi, S. Bianco, S. Colafranceschi[15], F. Fabbri, D. Piccolo

**INFN Sezione di Genova, Genova, Italy**
P. Fabbricatore, R. Musenich

**INFN Sezione di Milano-Biccoca [a], Università di Milano-Bicocca [b], Milano, Italy**
A. Benaglia[a,b], G.B. Cerati[a,b], F. De Guio[a,b,1], L. Di Matteo[a,b], A. Ghezzi[a,b,1], M. Malberti[a,b], S. Malvezzi[a], A. Martelli[a,b], A. Massironi[a,b], D. Menasce[a], L. Moroni[a], M. Paganoni[a,b], D. Pedrini[a], S. Ragazzi[a,b], N. Redaelli[a], S. Sala[a], T. Tabarelli de Fatis[a,b], V. Tancini[a,b]

**INFN Sezione di Napoli [a], Università di Napoli "Federico II" [b], Napoli, Italy**
S. Buontempo[a], C.A. Carrillo Montoya[a], A. Cimmino[a,b], A. De Cosa[a,b], M. De Gruttola[a,b], F. Fabozzi[a,16], A.O.M. Iorio[a], L. Lista[a], M. Merola[a,b], P. Noli[a,b], P. Paolucci[a]

**INFN Sezione di Padova [a], Università di Padova [b], Università di Trento (Trento) [c], Padova, Italy**
P. Azzi[a], N. Bacchetta[a], P. Bellan[a,b], D. Bisello[a,b], A. Branca[a], R. Carlin[a,b], P. Checchia[a], M. De Mattia[a,b], T. Dorigo[a], U. Dosselli[a], F. Fanzago[a], F. Gasparini[a,b], U. Gasparini[a,b], P. Giubilato[a,b], A. Gresele[a,c], S. Lacaprara[a,17], I. Lazzizzera[a,c], M. Margoni[a,b], M. Mazzucato[a], A.T. Meneguzzo[a,b], M. Nespolo[a], L. Perrozzi[a,1], N. Pozzobon[a,b], P. Ronchese[a,b], F. Simonetto[a,b], E. Torassa[a], M. Tosi[a,b], S. Vanini[a,b], P. Zotto[a,b], G. Zumerle[a,b]

**INFN Sezione di Pavia [a], Università di Pavia [b], Pavia, Italy**
P. Baesso[a,b], U. Berzano[a], C. Riccardi[a,b], P. Torre[a,b], P. Vitulo[a,b], C. Viviani[a,b]

**INFN Sezione di Perugia [a], Università di Perugia [b], Perugia, Italy**
M. Biasini[a,b], G.M. Bilei[a], B. Caponeri[a,b], L. Fanò[a,b], P. Lariccia[a,b], A. Lucaroni[a,b,1], G. Mantovani[a,b], M. Menichelli[a], A. Nappi[a,b], A. Santocchia[a,b], L. Servoli[a], S. Taroni[a,b], M. Valdata[a,b], R. Volpe[a,b,1]

**INFN Sezione di Pisa [a], Università di Pisa [b], Scuola Normale Superiore di Pisa [c], Pisa, Italy**
P. Azzurri[a,c], G. Bagliesi[a], J. Bernardini[a,b], T. Boccali[a,1], G. Broccolo[a,c], R. Castaldi[a], R.T. D'Agnolo[a,c], R. Dell'Orso[a], F. Fiori[a,b], L. Foà[a,c], A. Giassi[a], A. Kraan[a], F. Ligabue[a,c], T. Lomtadze[a], L. Martini[a], A. Messineo[a,b], F. Palla[a], F. Palmonari[a], S. Sarkar[a,c], G. Segneri[a], A.T. Serban[a], P. Spagnolo[a], R. Tenchini[a], G. Tonelli[a,b,1], A. Venturi[a,1], P.G. Verdini[a]

**INFN Sezione di Roma [a], Università di Roma "La Sapienza" [b], Roma, Italy**
L. Barone[a,b], F. Cavallari[a], D. Del Re[a,b], E. Di Marco[a,b], M. Diemoz[a], D. Franci[a,b], M. Grassi[a], E. Longo[a,b], G. Organtini[a,b], A. Palma[a,b], F. Pandolfi[a,b,1], R. Paramatti[a], S. Rahatlou[a,b]

**INFN Sezione di Torino [a], Università di Torino [b], Università del Piemonte Orientale (Novara) [c], Torino, Italy**
N. Amapane[a,b], R. Arcidiacono[a,c], S. Argiro[a,b], M. Arneodo[a,c], C. Biino[a], C. Botta[a,b,1], N. Cartiglia[a], R. Castello[a,b], M. Costa[a,b], N. Demaria[a], A. Graziano[a,b,1], C. Mariotti[a], M. Marone[a,b], S. Maselli[a], E. Migliore[a,b], G. Mila[a,b], V. Monaco[a,b], M. Musich[a,b], M.M. Obertino[a,c], N. Pastrone[a], M. Pelliccioni[a,b,1], A. Romero[a,b], M. Ruspa[a,c], R. Sacchi[a,b], V. Sola[a,b], A. Solano[a,b], A. Staiano[a], D. Trocino[a,b], A. Vilela Pereira[a,b,1]

**INFN Sezione di Trieste [a], Università di Trieste [b], Trieste, Italy**
F. Ambroglini[a,b], S. Belforte[a], F. Cossutti[a], G. Della Ricca[a,b], B. Gobbo[a], D. Montanino[a,b], A. Penzo[a]

**Kangwon National University, Chunchon, Korea**
S.G. Heo

**Kyungpook National University, Daegu, Korea**
S. Chang, J. Chung, D.H. Kim, G.N. Kim, J.E. Kim, D.J. Kong, H. Park, D. Son, D.C. Son

**Chonnam National University, Institute for Universe and Elementary Particles, Kwangju, Korea**
Zero Kim, J.Y. Kim, S. Song

**Korea University, Seoul, Korea**
S. Choi, B. Hong, M. Jo, H. Kim, J.H. Kim, T.J. Kim, K.S. Lee, D.H. Moon, S.K. Park, H.B. Rhee, E. Seo, S. Shin, K.S. Sim

**University of Seoul, Seoul, Korea**
M. Choi, S. Kang, H. Kim, C. Park, I.C. Park, S. Park, G. Ryu

**Sungkyunkwan University, Suwon, Korea**
Y. Choi, Y.K. Choi, J. Goh, J. Lee, S. Lee, H. Seo, I. Yu

**Vilnius University, Vilnius, Lithuania**
M.J. Bilinskas, I. Grigelionis, M. Janulis, D. Martisiute, P. Petrov, T. Sabonis

**Centro de Investigacion y de Estudios Avanzados del IPN, Mexico City, Mexico**
H. Castilla Valdez, E. De La Cruz Burelo, R. Lopez-Fernandez, A. Sánchez Hernández, L.M. Villasenor-Cendejas

**Universidad Iberoamericana, Mexico City, Mexico**
S. Carrillo Moreno, F. Vazquez Valencia

**Benemerita Universidad Autonoma de Puebla, Puebla, Mexico**
H.A. Salazar Ibarguen

**Universidad Autónoma de San Luis Potosí, San Luis Potosí, Mexico**
E. Casimiro Linares, A. Morelos Pineda, M.A. Reyes-Santos

**University of Auckland, Auckland, New Zealand**
P. Allfrey, D. Krofcheck

**University of Canterbury, Christchurch, New Zealand**
P.H. Butler, R. Doesburg, H. Silverwood

**National Centre for Physics, Quaid-I-Azam University, Islamabad, Pakistan**
M. Ahmad, I. Ahmed, M.I. Asghar, H.R. Hoorani, W.A. Khan, T. Khurshid, S. Qazi

**Institute of Experimental Physics, Faculty of Physics, University of Warsaw, Warsaw, Poland**
M. Cwiok, W. Dominik, K. Doroba, A. Kalinowski, M. Konecki, J. Krolikowski

**Soltan Institute for Nuclear Studies, Warsaw, Poland**
T. Frueboes, R. Gokieli, M. Górski, M. Kazana, K. Nawrocki, K. Romanowska-Rybinska, M. Szleper, G. Wrochna, P. Zalewski

**Laboratório de Instrumentação e Física Experimental de Partículas, Lisboa, Portugal**
N. Almeida, A. David, P. Faccioli, P.G. Ferreira Parracho, M. Gallinaro, P. Martins, P. Musella, A. Nayak, P.Q. Ribeiro, J. Seixas, P. Silva, J. Varela[1], H.K. Wöhri

**Joint Institute for Nuclear Research, Dubna, Russia**
I. Belotelov, P. Bunin, M. Finger, M. Finger Jr., I. Golutvin, A. Kamenev, V. Karjavin, G. Kozlov, A. Lanev, P. Moisenz, V. Palichik, V. Perelygin, S. Shmatov, V. Smirnov, A. Volodko, A. Zarubin

**Petersburg Nuclear Physics Institute, Gatchina (St Petersburg), Russia**
N. Bondar, V. Golovtsov, Y. Ivanov, V. Kim, P. Levchenko, V. Murzin, V. Oreshkin, I. Smirnov, V. Sulimov, L. Uvarov, S. Vavilov, A. Vorobyev

**Institute for Nuclear Research, Moscow, Russia**
Yu. Andreev, S. Gninenko, N. Golubev, M. Kirsanov, N. Krasnikov, V. Matveev, A. Pashenkov, A. Toropin, S. Troitsky

**Institute for Theoretical and Experimental Physics, Moscow, Russia**
V. Epshteyn, V. Gavrilov, V. Kaftanov†, M. Kossov[1], A. Krokhotin, N. Lychkovskaya, G. Safronov, S. Semenov, V. Stolin, E. Vlasov, A. Zhokin

**Moscow State University, Moscow, Russia**
E. Boos, M. Dubinin[18], L. Dudko, A. Ershov, A. Gribushin, O. Kodolova, I. Lokhtin, S. Obraztsov, S. Petrushanko, L. Sarycheva, V. Savrin, A. Snigirev

**P.N. Lebedev Physical Institute, Moscow, Russia**
V. Andreev, M. Azarkin, I. Dremin, M. Kirakosyan, S.V. Rusakov, A. Vinogradov

**State Research Center of Russian Federation, Institute for High Energy Physics, Protvino, Russia**
I. Azhgirey, S. Bitioukov, V. Grishin[1], V. Kachanov, D. Konstantinov, A. Korablev, V. Krychkine, V. Petrov, R. Ryutin, S. Slabospitsky, A. Sobol, L. Tourtchanovitch, S. Troshin, N. Tyurin, A. Uzunian, A. Volkov

**University of Belgrade, Faculty of Physics and Vinca Institute of Nuclear Sciences, Belgrade, Serbia**
P. Adzic[19], M. Djordjevic, D. Krpic[19], J. Milosevic

**Centro de Investigaciones Energéticas Medioambientales y Tecnológicas (CIEMAT), Madrid, Spain**
M. Aguilar-Benitez, J. Alcaraz Maestre, P. Arce, C. Battilana, E. Calvo, M. Cepeda, M. Cerrada, N. Colino, B. De La Cruz, C. Diez Pardos, C. Fernandez Bedoya, J.P. Fernández Ramos, A. Ferrando, J. Flix, M.C. Fouz, P. Garcia-Abia, O. Gonzalez Lopez, S. Goy Lopez, J.M. Hernandez, M.I. Josa, G. Merino, J. Puerta Pelayo, I. Redondo, L. Romero, J. Santaolalla, M.S. Soares, C. Willmott

**Universidad Autónoma de Madrid, Madrid, Spain**
C. Albajar, G. Codispoti, J.F. de Trocóniz

**Universidad de Oviedo, Oviedo, Spain**
J. Cuevas, J. Fernandez Menendez, S. Folgueras, I. Gonzalez Caballero, L. Lloret Iglesias, J.M. Vizan Garcia

**Instituto de Física de Cantabria (IFCA), CSIC-Universidad de Cantabria, Santander, Spain**
J.A. Brochero Cifuentes, I.J. Cabrillo, A. Calderon, M. Chamizo Llatas, S.H. Chuang, J. Duarte Campderros, M. Felcini[20], M. Fernandez, G. Gomez, J. Gonzalez Sanchez, C. Jorda, P. Lobelle Pardo, A. Lopez Virto, J. Marco, R. Marco, C. Martinez Rivero, F. Matorras, F.J. Munoz Sanchez, J. Piedra Gomez[21], T. Rodrigo, A. Ruiz Jimeno, L. Scodellaro, M. Sobron Sanudo, I. Vila, R. Vilar Cortabitarte

**CERN, European Organization for Nuclear Research, Geneva, Switzerland**
D. Abbaneo, E. Auffray, G. Auzinger, P. Baillon, A.H. Ball, D. Barney, A.J. Bell[22], D. Benedetti, C. Bernet[3], W. Bialas, P. Bloch, A. Bocci, S. Bolognesi, H. Breuker, G. Brona, K. Bunkowski, T. Camporesi, E. Cano, G. Cerminara, T. Christiansen, J.A. Coarasa Perez, B. Curé, D. D'Enterria, A. De Roeck, F. Duarte Ramos, A. Elliott-Peisert, B. Frisch, W. Funk, A. Gaddi, S. Gennai, G. Georgiou, H. Gerwig, D. Gigi, K. Gill, D. Giordano, F. Glege, R. Gomez-Reino Garrido, M. Gouzevitch, P. Govoni, S. Gowdy, L. Guiducci, M. Hansen, J. Harvey, J. Hegeman, B. Hegner, C. Henderson, G. Hesketh, H.F. Hoffmann, A. Honma, V. Innocente, P. Janot, E. Karavakis, P. Lecoq, C. Leonidopoulos, C. Lourenço, A. Macpherson, T. Mäki, L. Malgeri, M. Mannelli, L. Masetti, F. Meijers, S. Mersi, E. Meschi, R. Moser, M.U. Mozer, M. Mulders, E. Nesvold[1], M. Nguyen, T. Orimoto, L. Orsini, E. Perez, A. Petrilli, A. Pfeiffer, M. Pierini, M. Pimiä, G. Polese, A. Racz, G. Rolandi[23], T. Rommerskirchen, C. Rovelli[24], M. Rovere, H. Sakulin, C. Schäfer, C. Schwick, I. Segoni, A. Sharma, P. Siegrist, M. Simon, P. Sphicas[25], D. Spiga, M. Spiropulu[18], F. Stöckli, M. Stoye, P. Tropea, A. Tsirou, A. Tsyganov, G.I. Veres[12], P. Vichoudis, M. Voutilainen, W.D. Zeuner

**Paul Scherrer Institut, Villigen, Switzerland**
W. Bertl, K. Deiters, W. Erdmann, K. Gabathuler, R. Horisberger, Q. Ingram, H.C. Kaestli, S. König, D. Kotlinski, U. Langenegger, F. Meier, D. Renker, T. Rohe, J. Sibille[26], A. Starodumov[27]

**Institute for Particle Physics, ETH Zurich, Zurich, Switzerland**
P. Bortignon, L. Caminada[28], Z. Chen, S. Cittolin, G. Dissertori, M. Dittmar, J. Eugster, K. Freudenreich, C. Grab, A. Hervé, W. Hintz, P. Lecomte, W. Lustermann, C. Marchica[28], P. Martinez Ruiz del Arbol, P. Meridiani, P. Milenovic[29], F. Moortgat, P. Nef, F. Nessi-Tedaldi, L. Pape, F. Pauss, T. Punz, A. Rizzi, F.J. Ronga, M. Rossini, L. Sala, A.K. Sanchez, M.-C. Sawley, B. Stieger, L. Tauscher†, A. Thea, K. Theofilatos, D. Treille, C. Urscheler, R. Wallny[20], M. Weber, L. Wehrli, J. Weng

**Universität Zürich, Zurich, Switzerland**
E. Aguiló, C. Amsler, V. Chiochia, S. De Visscher, C. Favaro, M. Ivova Rikova, B. Millan Mejias, C. Regenfus, P. Robmann, A. Schmidt, H. Snoek, L. Wilke

**National Central University, Chung-Li, Taiwan**
Y.H. Chang, K.H. Chen, W.T. Chen, S. Dutta, A. Go, C.M. Kuo, S.W. Li, W. Lin, M.H. Liu, Z.K. Liu, Y.J. Lu, J.H. Wu, S.S. Yu

**National Taiwan University (NTU), Taipei, Taiwan**
P. Bartalini, P. Chang, Y.H. Chang, Y.W. Chang, Y. Chao, K.F. Chen, W.-S. Hou, Y. Hsiung, K.Y. Kao, Y.J. Lei, R.-S. Lu, J.G. Shiu, Y.M. Tzeng, M. Wang

**Cukurova University, Adana, Turkey**
A. Adiguzel, M.N. Bakirci, S. Cerci[30], C. Dozen, I. Dumanoglu, E. Eskut, S. Girgis, G. Gokbulut, Y. Guler, E. Gurpinar, I. Hos, E.E. Kangal, T. Karaman, A. Kayis Topaksu, A. Nart, G. Onengut, K. Ozdemir, S. Ozturk, A. Polatoz, K. Sogut[31], B. Tali, H. Topakli, D. Uzun, L.N. Vergili, M. Vergili, C. Zorbilmez

**Middle East Technical University, Physics Department, Ankara, Turkey**
I.V. Akin, T. Aliev, S. Bilmis, M. Deniz, H. Gamsizkan, A.M. Guler, K. Ocalan, A. Ozpineci, M. Serin, R. Sever, U.E. Surat, E. Yildirim, M. Zeyrek

**Bogazici University, Istanbul, Turkey**
M. Deliomeroglu, D. Demir[32], E. Gülmez, A. Halu, B. Isildak, M. Kaya[33], O. Kaya[33], S. Ozkorucuklu[34], N. Sonmez[35]

**National Scientific Center, Kharkov Institute of Physics and Technology, Kharkov, Ukraine**
L. Levchuk

**University of Bristol, Bristol, United Kingdom**
P. Bell, F. Bostock, J.J. Brooke, T.L. Cheng, E. Clement, D. Cussans, R. Frazier, J. Goldstein, M. Grimes, M. Hansen, D. Hartley, G.P. Heath, H.F. Heath, B. Huckvale, J. Jackson, L. Kreczko, S. Metson, D.M. Newbold[36], K. Nirunpong, A. Poll, S. Senkin, V.J. Smith, S. Ward

**Rutherford Appleton Laboratory, Didcot, United Kingdom**
L. Basso, K.W. Bell, A. Belyaev, C. Brew, R.M. Brown, B. Camanzi, D.J.A. Cockerill, J.A. Coughlan, K. Harder, S. Harper, B.W. Kennedy, E. Olaiya, D. Petyt, B.C. Radburn-Smith, C.H. Shepherd-Themistocleous, I.R. Tomalin, W.J. Womersley, S.D. Worm

**Imperial College, London, United Kingdom**
R. Bainbridge, G. Ball, J. Ballin, R. Beuselinck, O. Buchmuller, D. Colling, N. Cripps, M. Cutajar, G. Davies, M. Della Negra, J. Fulcher, D. Futyan, A. Guneratne Bryer, G. Hall, Z. Hatherell, J. Hays, G. Iles, G. Karapostoli, L. Lyons, A.-M. Magnan, J. Marrouche, R. Nandi, J. Nash, A. Nikitenko[27], A. Papageorgiou, M. Pesaresi, K. Petridis, M. Pioppi[37], D.M. Raymond, N. Rompotis, A. Rose, M.J. Ryan, C. Seez, P. Sharp, A. Sparrow, A. Tapper, S. Tourneur, M. Vazquez Acosta, T. Virdee, S. Wakefield, D. Wardrope, T. Whyntie

**Brunel University, Uxbridge, United Kingdom**
M. Barrett, M. Chadwick, J.E. Cole, P.R. Hobson, A. Khan, P. Kyberd, D. Leslie, W. Martin, I.D. Reid, L. Teodorescu

**Baylor University, Waco, USA**
K. Hatakeyama

**Boston University, Boston, USA**
T. Bose, E. Carrera Jarrin, A. Clough, C. Fantasia, A. Heister, J. St. John, P. Lawson, D. Lazic, J. Rohlf, D. Sperka, L. Sulak

**Brown University, Providence, USA**
A. Avetisyan, S. Bhattacharya, J.P. Chou, D. Cutts, A. Ferapontov, U. Heintz, S. Jabeen, G. Kukartsev, G. Landsberg, M. Narain, D. Nguyen, M. Segala, T. Speer, K.V. Tsang

**University of California, Davis, Davis, USA**
M.A. Borgia, R. Breedon, M. Calderon De La Barca Sanchez, D. Cebra, S. Chauhan, M. Chertok, J. Conway, P.T. Cox, J. Dolen, R. Erbacher, E. Friis, W. Ko, A. Kopecky, R. Lander, H. Liu, S. Maruyama, T. Miceli, M. Nikolic, D. Pellett, J. Robles, T. Schwarz, M. Searle, J. Smith, M. Squires, M. Tripathi, R. Vasquez Sierra, C. Veelken

**University of California, Los Angeles, Los Angeles, USA**
V. Andreev, K. Arisaka, D. Cline, R. Cousins, A. Deisher, J. Duris, S. Erhan[1], C. Farrell, J. Hauser, M. Ignatenko, C. Jarvis, C. Plager, G. Rakness, P. Schlein†, J. Tucker, V. Valuev

**University of California, Riverside, Riverside, USA**
J. Babb, R. Clare, J. Ellison, J.W. Gary, F. Giordano, G. Hanson, G.Y. Jeng, S.C. Kao, F. Liu, H. Liu, A. Luthra, H. Nguyen, G. Pasztor[38], A. Satpathy, B.C. Shen†, R. Stringer, J. Sturdy, S. Sumowidagdo, R. Wilken, S. Wimpenny

**University of California, San Diego, La Jolla, USA**
W. Andrews, J.G. Branson, E. Dusinberre, D. Evans, F. Golf, A. Holzner, R. Kelley, M. Lebourgeois, J. Letts, B. Mangano, J. Muelmenstaedt, S. Padhi, C. Palmer, G. Petrucciani, H. Pi, M. Pieri, R. Ranieri, M. Sani, V. Sharma[1], S. Simon, Y. Tu, A. Vartak, F. Würthwein, A. Yagil

**University of California, Santa Barbara, Santa Barbara, USA**
D. Barge, R. Bellan, C. Campagnari, M. D'Alfonso, T. Danielson, K. Flowers, P. Geffert, J. Incandela, C. Justus, P. Kalavase, S.A. Koay, D. Kovalskyi, V. Krutelyov, S. Lowette, N. Mccoll, V. Pavlunin, F. Rebassoo, J. Ribnik, J. Richman, R. Rossin, D. Stuart, W. To, J.R. Vlimant

**California Institute of Technology, Pasadena, USA**
A. Bornheim, J. Bunn, Y. Chen, M. Gataullin, D. Kcira, V. Litvine, Y. Ma, A. Mott, H.B. Newman, C. Rogan, V. Timciuc, P. Traczyk, J. Veverka, R. Wilkinson, Y. Yang, R.Y. Zhu

**Carnegie Mellon University, Pittsburgh, USA**
B. Akgun, R. Carroll, T. Ferguson, Y. Iiyama, D.W. Jang, S.Y. Jun, Y.F. Liu, M. Paulini, J. Russ, N. Terentyev, H. Vogel, I. Vorobiev

**University of Colorado at Boulder, Boulder, USA**
J.P. Cumalat, M.E. Dinardo, B.R. Drell, C.J. Edelmaier, W.T. Ford, B. Heyburn, E. Luiggi Lopez, U. Nauenberg, J.G. Smith, K. Stenson, K.A. Ulmer, S.R. Wagner, S.L. Zang

**Cornell University, Ithaca, USA**
L. Agostino, J. Alexander, A. Chatterjee, S. Das, N. Eggert, L.J. Fields, L.K. Gibbons, B. Heltsley, W. Hopkins, A. Khukhunaishvili, B. Kreis, V. Kuznetsov, G. Nicolas Kaufman, J.R. Patterson, D. Puigh, D. Riley, A. Ryd, X. Shi, W. Sun, W.D. Teo, J. Thom, J. Thompson, J. Vaughan, Y. Weng, L. Winstrom, P. Wittich

**Fairfield University, Fairfield, USA**
A. Biselli, G. Cirino, D. Winn

**Fermi National Accelerator Laboratory, Batavia, USA**
S. Abdullin, M. Albrow, J. Anderson, G. Apollinari, M. Atac, J.A. Bakken, S. Banerjee, L.A.T. Bauerdick, A. Beretvas, J. Berryhill, P.C. Bhat, I. Bloch, F. Borcherding, K. Burkett, J.N. Butler, V. Chetluru, H.W.K. Cheung, F. Chlebana, S. Cihangir, M. Demarteau, D.P. Eartly, V.D. Elvira, S. Esen, I. Fisk, J. Freeman, Y. Gao, E. Gottschalk, D. Green, K. Gunthoti, O. Gutsche, A. Hahn, J. Hanlon, R.M. Harris, J. Hirschauer, B. Hooberman, E. James, H. Jensen, M. Johnson, U. Joshi, R. Khatiwada, B. Kilminster, B. Klima, K. Kousouris, S. Kunori, S. Kwan, P. Limon, R. Lipton, J. Lykken, K. Maeshima, J.M. Marraffino, D. Mason, P. McBride, T. McCauley, T. Miao, K. Mishra, S. Mrenna, Y. Musienko[39], C. Newman-Holmes, V. O'Dell, S. Popescu[40], R. Pordes, O. Prokofyev, N. Saoulidou, E. Sexton-Kennedy, S. Sharma, A. Soha, W.J. Spalding, L. Spiegel, P. Tan, L. Taylor, S. Tkaczyk, L. Uplegger, E.W. Vaandering, R. Vidal, J. Whitmore, W. Wu, F. Yang, F. Yumiceva, J.C. Yun

**University of Florida, Gainesville, USA**
D. Acosta, P. Avery, D. Bourilkov, M. Chen, G.P. Di Giovanni, D. Dobur, A. Drozdetskiy, R.D. Field, M. Fisher, Y. Fu, I.K. Furic, J. Gartner, S. Goldberg, B. Kim, S. Klimenko, J. Konigsberg, A. Korytov, A. Kropivnitskaya, T. Kypreos, K. Matchev, G. Mitselmakher, L. Muniz, Y. Pakhotin, C. Prescott, R. Remington, M. Schmitt, B. Scurlock, P. Sellers, N. Skhirtladze, D. Wang, J. Yelton, M. Zakaria

**Florida International University, Miami, USA**
C. Ceron, V. Gaultney, L. Kramer, L.M. Lebolo, S. Linn, P. Markowitz, G. Martinez, J.L. Rodriguez

**Florida State University, Tallahassee, USA**
T. Adams, A. Askew, D. Bandurin, J. Bochenek, J. Chen, B. Diamond, S.V. Gleyzer, J. Haas, S. Hagopian, V. Hagopian, M. Jenkins, K.F. Johnson, H. Prosper, S. Sekmen, V. Veeraraghavan

**Florida Institute of Technology, Melbourne, USA**
M.M. Baarmand, B. Dorney, S. Guragain, M. Hohlmann, H. Kalakhety, R. Ralich, I. Vodopiyanov

**University of Illinois at Chicago (UIC), Chicago, USA**
M.R. Adams, I.M. Anghel, L. Apanasevich, Y. Bai, V.E. Bazterra, R.R. Betts, J. Callner, R. Cavanaugh, C. Dragoiu, E.J. Garcia-Solis, C.E. Gerber, D.J. Hofman, S. Khalatyan, F. Lacroix, C. O'Brien, C. Silvestre, A. Smoron, D. Strom, N. Varelas

**The University of Iowa, Iowa City, USA**
U. Akgun, E.A. Albayrak, B. Bilki, K. Cankocak[41], W. Clarida, F. Duru, C.K. Lae, E. McCliment, J.-P. Merlo, H. Mermerkaya, A. Mestvirishvili, A. Moeller, J. Nachtman, C.R. Newsom, E. Norbeck, J. Olson, Y. Onel, F. Ozok, S. Sen, J. Wetzel, T. Yetkin, K. Yi

**Johns Hopkins University, Baltimore, USA**
B.A. Barnett, B. Blumenfeld, A. Bonato, C. Eskew, D. Fehling, G. Giurgiu, A.V. Gritsan, Z.J. Guo, G. Hu, P. Maksimovic, S. Rappoccio, M. Swartz, N.V. Tran, A. Whitbeck

**The University of Kansas, Lawrence, USA**
P. Baringer, A. Bean, G. Benelli, O. Grachov, M. Murray, D. Noonan, V. Radicci, S. Sanders, J.S. Wood, V. Zhukova

**Kansas State University, Manhattan, USA**
T. Bolton, I. Chakaberia, A. Ivanov, M. Makouski, Y. Maravin, S. Shrestha, I. Svintradze, Z. Wan

**Lawrence Livermore National Laboratory, Livermore, USA**
J. Gronberg, D. Lange, D. Wright

**University of Maryland, College Park, USA**
A. Baden, M. Boutemeur, S.C. Eno, D. Ferencek, J.A. Gomez, N.J. Hadley, R.G. Kellogg, M. Kirn, Y. Lu, A.C. Mignerey, K. Rossato, P. Rumerio, F. Santanastasio, A. Skuja, J. Temple, M.B. Tonjes, S.C. Tonwar, E. Twedt

**Massachusetts Institute of Technology, Cambridge, USA**
B. Alver, G. Bauer, J. Bendavid, W. Busza, E. Butz, I.A. Cali, M. Chan, V. Dutta, P. Everaerts, G. Gomez Ceballos, M. Goncharov, K.A. Hahn, P. Harris, Y. Kim, M. Klute, Y.-J. Lee, W. Li, C. Loizides, P.D. Luckey, T. Ma, S. Nahn, C. Paus, D. Ralph, C. Roland, G. Roland, M. Rudolph, G.S.F. Stephans, K. Sumorok, K. Sung, E.A. Wenger, S. Xie, M. Yang, Y. Yilmaz, A.S. Yoon, M. Zanetti

**University of Minnesota, Minneapolis, USA**
P. Cole, S.I. Cooper, P. Cushman, B. Dahmes, A. De Benedetti, P.R. Dudero, G. Franzoni, J. Haupt, K. Klapoetke, Y. Kubota, J. Mans, V. Rekovic, R. Rusack, M. Sasseville, A. Singovsky

**University of Mississippi, University, USA**
L.M. Cremaldi, R. Godang, R. Kroeger, L. Perera, R. Rahmat, D.A. Sanders, D. Summers

**University of Nebraska-Lincoln, Lincoln, USA**
K. Bloom, S. Bose, J. Butt, D.R. Claes, A. Dominguez, M. Eads, J. Keller, T. Kelly, I. Kravchenko, J. Lazo-Flores, C. Lundstedt, H. Malbouisson, S. Malik, G.R. Snow

**State University of New York at Buffalo, Buffalo, USA**
U. Baur, A. Godshalk, I. Iashvili, A. Kharchilava, A. Kumar, S.P. Shipkowski, K. Smith

**Northeastern University, Boston, USA**
G. Alverson, E. Barberis, D. Baumgartel, O. Boeriu, M. Chasco, K. Kaadze, S. Reucroft, J. Swain, D. Wood, J. Zhang

**Northwestern University, Evanston, USA**
A. Anastassov, A. Kubik, N. Odell, R.A. Ofierzynski, B. Pollack, A. Pozdnyakov, M. Schmitt, S. Stoynev, M. Velasco, S. Won

**University of Notre Dame, Notre Dame, USA**
L. Antonelli, D. Berry, M. Hildreth, C. Jessop, D.J. Karmgard, J. Kolb, T. Kolberg, K. Lannon, W. Luo, S. Lynch, N. Marinelli, D.M. Morse, T. Pearson, R. Ruchti, J. Slaunwhite, N. Valls, J. Warchol, M. Wayne, J. Ziegler

**The Ohio State University, Columbus, USA**
B. Bylsma, L.S. Durkin, J. Gu, C. Hill, P. Killewald, K. Kotov, T.Y. Ling, M. Rodenburg, G. Williams

**Princeton University, Princeton, USA**
N. Adam, E. Berry, P. Elmer, D. Gerbaudo, V. Halyo, P. Hebda, A. Hunt, J. Jones, E. Laird, D. Lopes Pegna, D. Marlow, T. Medvedeva, M. Mooney, J. Olsen, P. Piroué, X. Quan, H. Saka, D. Stickland, C. Tully, J.S. Werner, A. Zuranski

**University of Puerto Rico, Mayaguez, USA**
J.G. Acosta, X.T. Huang, A. Lopez, H. Mendez, S. Oliveros, J.E. Ramirez Vargas, A. Zatserklyaniy

**Purdue University, West Lafayette, USA**
E. Alagoz, V.E. Barnes, G. Bolla, L. Borrello, D. Bortoletto, A. Everett, A.F. Garfinkel, Z. Gecse, L. Gutay, Z. Hu, M. Jones, O. Koybasi, A.T. Laasanen, N. Leonardo, C. Liu, V. Maroussov, P. Merkel, D.H. Miller, N. Neumeister, K. Potamianos, I. Shipsey, D. Silvers, A. Svyatkovskiy, H.D. Yoo, J. Zablocki, Y. Zheng

**Purdue University Calumet, Hammond, USA**
P. Jindal, N. Parashar

**Rice University, Houston, USA**
C. Boulahouache, V. Cuplov, K.M. Ecklund, F.J.M. Geurts, J.H. Liu, J. Morales, B.P. Padley, R. Redjimi, J. Roberts, J. Zabel

**University of Rochester, Rochester, USA**
B. Betchart, A. Bodek, Y.S. Chung, R. Covarelli, P. de Barbaro, R. Demina, Y. Eshaq, H. Flacher,

A. Garcia-Bellido, P. Goldenzweig, Y. Gotra, J. Han, A. Harel, D.C. Miner, D. Orbaker, G. Petrillo, D. Vishnevskiy, M. Zielinski

**The Rockefeller University, New York, USA**
A. Bhatti, L. Demortier, K. Goulianos, G. Lungu, C. Mesropian, M. Yan

**Rutgers, the State University of New Jersey, Piscataway, USA**
O. Atramentov, A. Barker, D. Duggan, Y. Gershtein, R. Gray, E. Halkiadakis, D. Hidas, D. Hits, A. Lath, S. Panwalkar, R. Patel, A. Richards, K. Rose, S. Schnetzer, S. Somalwar, R. Stone, S. Thomas

**University of Tennessee, Knoxville, USA**
G. Cerizza, M. Hollingsworth, S. Spanier, Z.C. Yang, A. York

**Texas A&M University, College Station, USA**
J. Asaadi, R. Eusebi, J. Gilmore, A. Gurrola, T. Kamon, V. Khotilovich, R. Montalvo, C.N. Nguyen, J. Pivarski, A. Safonov, S. Sengupta, A. Tatarinov, D. Toback, M. Weinberger

**Texas Tech University, Lubbock, USA**
N. Akchurin, C. Bardak, J. Damgov, C. Jeong, K. Kovitanggoon, S.W. Lee, P. Mane, Y. Roh, A. Sill, I. Volobouev, R. Wigmans, E. Yazgan

**Vanderbilt University, Nashville, USA**
E. Appelt, E. Brownson, D. Engh, C. Florez, W. Gabella, W. Johns, P. Kurt, C. Maguire, A. Melo, P. Sheldon, J. Velkovska

**University of Virginia, Charlottesville, USA**
M.W. Arenton, M. Balazs, S. Boutle, M. Buehler, S. Conetti, B. Cox, B. Francis, R. Hirosky, A. Ledovskoy, C. Lin, C. Neu, R. Yohay

**Wayne State University, Detroit, USA**
S. Gollapinni, R. Harr, P.E. Karchin, P. Lamichhane, M. Mattson, C. Milstène, A. Sakharov

**University of Wisconsin, Madison, USA**
M. Anderson, M. Bachtis, J.N. Bellinger, D. Carlsmith, S. Dasu, J. Efron, L. Gray, K.S. Grogg, M. Grothe, R. Hall-Wilton[1], M. Herndon, P. Klabbers, J. Klukas, A. Lanaro, C. Lazaridis, J. Leonard, D. Lomidze, R. Loveless, A. Mohapatra, D. Reeder, I. Ross, A. Savin, W.H. Smith, J. Swanson, M. Weinberg

†: Deceased
1: Also at CERN, European Organization for Nuclear Research, Geneva, Switzerland
2: Also at Universidade Federal do ABC, Santo Andre, Brazil
3: Also at Laboratoire Leprince-Ringuet, Ecole Polytechnique, IN2P3-CNRS, Palaiseau, France
4: Also at Suez Canal University, Suez, Egypt
5: Also at Fayoum University, El-Fayoum, Egypt
6: Also at Soltan Institute for Nuclear Studies, Warsaw, Poland
7: Also at Massachusetts Institute of Technology, Cambridge, USA
8: Also at Université de Haute-Alsace, Mulhouse, France
9: Also at Brandenburg University of Technology, Cottbus, Germany
10: Also at Moscow State University, Moscow, Russia
11: Also at Institute of Nuclear Research ATOMKI, Debrecen, Hungary
12: Also at Eötvös Loránd University, Budapest, Hungary
13: Also at Tata Institute of Fundamental Research - HECR, Mumbai, India
14: Also at University of Visva-Bharati, Santiniketan, India

15: Also at Facoltà Ingegneria Università di Roma "La Sapienza", Roma, Italy
16: Also at Università della Basilicata, Potenza, Italy
17: Also at Laboratori Nazionali di Legnaro dell' INFN, Legnaro, Italy
18: Also at California Institute of Technology, Pasadena, USA
19: Also at Faculty of Physics of University of Belgrade, Belgrade, Serbia
20: Also at University of California, Los Angeles, Los Angeles, USA
21: Also at University of Florida, Gainesville, USA
22: Also at Université de Genève, Geneva, Switzerland
23: Also at Scuola Normale e Sezione dell' INFN, Pisa, Italy
24: Also at INFN Sezione di Roma; Università di Roma "La Sapienza", Roma, Italy
25: Also at University of Athens, Athens, Greece
26: Also at The University of Kansas, Lawrence, USA
27: Also at Institute for Theoretical and Experimental Physics, Moscow, Russia
28: Also at Paul Scherrer Institut, Villigen, Switzerland
29: Also at University of Belgrade, Faculty of Physics and Vinca Institute of Nuclear Sciences, Belgrade, Serbia
30: Also at Adiyaman University, Adiyaman, Turkey
31: Also at Mersin University, Mersin, Turkey
32: Also at Izmir Institute of Technology, Izmir, Turkey
33: Also at Kafkas University, Kars, Turkey
34: Also at Suleyman Demirel University, Isparta, Turkey
35: Also at Ege University, Izmir, Turkey
36: Also at Rutherford Appleton Laboratory, Didcot, United Kingdom
37: Also at INFN Sezione di Perugia; Università di Perugia, Perugia, Italy
38: Also at KFKI Research Institute for Particle and Nuclear Physics, Budapest, Hungary
39: Also at Institute for Nuclear Research, Moscow, Russia
40: Also at Horia Hulubei National Institute of Physics and Nuclear Engineering (IFIN-HH), Bucharest, Romania
41: Also at Istanbul Technical University, Istanbul, Turkey